REVISTA MEXICANA DE CIENCIAS GEOLÓGICAS

Revista Mexicana de Ciencias Geológicas, v. 42, num. 3, December 2025, p. 124–144 ISSN-L 2007-2902 https://rmcg.unam.mx

Type: Original research



Geothermobarometry, structure, and geochronology of low-grade rocks in the southern Acatlán Complex, San Martín Zacatepec, Oaxaca

Anthony Ramírez-Salazar^{1,*}, Joseph U. Chaverria-Urrieta², and Rodrigo Gutiérrez-Navarro³

¹Instituto de Geología, Universidad Nacional Autónoma de México, Ciudad Universitaria 04510, Mexico City, Mexico. ²Escuela Nacional de Ciencias de la Tierra, Universidad Nacional Autónoma de México, Ciudad Universitaria 04510, Mexico City, Mexico. ³Facultad de Ingeniería, Universidad Nacional Autónoma de México, Ciudad Universitaria 04510, Mexico City, Mexico.

> * Corresponding author (A. Ramírez-Salazar): anthony@geologia.unam.mx; r.s.anthonyy@gmail.com https://orcid.org/0000-0001-8948-8206

EDITORS:

Natalia Pardo Villaveces Luigi A. Solari

How to cite:

Ramírez-Salazar, A., Chaverria-Urrieta, J. U., Gutiérrez-Navarro, R. (2025). Geothermobarometry, structure, and geochronology of low-grade rocks in the southern Acatlán Complex, San Martín Zacatepec, Oaxaca. *Revista Mexicana de Ciencias Geológicas*, 42(3), 124–144. DOI: https://dx.doi. org/10.22201/igc.20072902e.2025.3.1883

Manuscript received: June 12, 2025 Corrected manuscript received: August 30, 2025 Manuscript accepted: August 31, 2025 Published Online: December 1, 2025

COPYRIGHT

© 2025 The Author(s).

This is an open-access article published and distributed by the Universidad Nacional Autónoma de México under the terms of a <u>Creative Commons Attribution 4.0 International License (CC BY)</u> which permits unrestricted use, distribution, and reproduction in any medium, provided the original author and source are credited.



ABSTRACT

The Acatlán Complex (AC) in southern Mexico is a critical lithodemic province for Paleozoic paleoreconstructions. It is mainly composed of low-grade volcano-sedimentary sequences, yet quantitative geothermobarometric data are scarce in the literature, and the southern-central portions remain poorly described. This lack of information hinders our ability to refine the geological history of the AC. In this study, we investigate the San Martín Zacatepec area in the state of Oaxaca, Mexico, where low-grade rocks are in contact with Esperanza metagranitoids along a mylonitic normal fault. We present new structural and petrological data, phase equilibria modeling results, and U-Pb geochronological data for the Zacatepec low-grade rocks (ZLGR), as well as petrological and geochronological data for the associated metagranitoids. Our data show that the ZLGR were deposited in a submarine environment, with a Mississippian (334 ± 8.9 Ma) maximum depositional age, and major detrital zircon populations at ca. 540, 910, 1100, and 1900 Ma. The ZLGR later underwent two deformation events (D_{LG1-2}), evolving from 0.15-0.27 GPa and 420-450 °C to 0.45-0.65 GPa and 480-540 °C, which produced foliations (S_{LG1-2}) and isoclinal folds (F_{LG2}). A third deformation episode generated upright open folds (F_{LG3}). The geological characteristics of the ZLGR indicate that they belong to the pre-Pennsylvanian low-grade rocks (PPLGR) that comprise most of the AC. The associated metagranitoids display inherited zircon populations at ca. 1100, 1200, and 1400 Ma, and have a peraluminous nature typical of felsic melts derived from crustal partial melting. Our results support paleogeographic models linking the AC to Oaxaquia and western Gondwana. However, our zircon data suggest that the source of the detrital and inherited zircon populations may have been the recently identified Oaxaquia-related metamorphic terranes in southern Mexico, rather than the traditionally inferred Oaxacan Complex. We additionally propose that the metamorphic evolution recorded during D_{LG1-2} is consistent with tectonic models that attribute this deformation to the exhumation and overthrusting of high-pressure rocks of the AC over the PPLGR. The new data from the Zacatepec area provide valuable insights into the evolution of the PPLGR and the Esperanza granitoids in the AC and may serve as a reference for comparative studies across the complex and for interpreting its geological and tectonic history.

Keywords: Low-grade metamorphism; metragranitoids; phase equilibria modeling; geothermobarometry; U-Pb zircon geochronology; Acatlán Complex; Mexico.



RESUMEN

El Complejo Acatlán (CA) en el sur de México es una provincia litodémica clave para las paleo-reconstrucciones del Paleozoico. Está compuesto principalmente por secuencias volcano-sedimentarias de bajo grado, pero los datos geotermobarométricos cuantitativos son escasos en la literatura, y las porciones centro-sur aún no han sido descritas a detalle. Esta falta de información limita nuestra capacidad para refinar la historia geológica del CA. En este estudio, investigamos el área de San Martín Zacatepec, en el estado de Oaxaca, México, donde las rocas de bajo grado están en contacto con metagranitoides Esperanza a lo largo de una falla normal milonítica. Presentamos nuevos datos estructurales y petrológicos, modelado de equilibrios de fases y datos geocronológicos U-Pb para las rocas de bajo grado de Zacatepec (RBGZ), así como datos petrológicos y geocronológicos de los metagranitoides asociados. Nuestros datos muestran que las RBGZ fueron depositadas en un ambiente submarino, con una edad máxima de depósito misisipíca (334 ± 8.9 Ma), y poblaciones principales de circones detríticos ca. 540, 910, 1100 y 1900 Ma. Posteriormente, las RBGZ experimentaron dos eventos de deformación (D_{LGI-2}), evolucionando de 0.15–0.27 GPa y 420-450 °C a 0.45-0.65 GPa y 480-540 °C, lo que generó foliaciones (S_{LGI-2}) y pliegues isoclinales (F_{LG2}). Un tercer episodio de deformación generó pliegues abiertos hacia arriba (F_{LG3}). Las características geológicas de las RBGZ indican que forman parte de las rocas de bajo grado pre-Pensilvanianas (RBGPP) que componen la mayor parte del CA. Los metagranitoides asociados muestran poblaciones heredadas de circones en ca. 1100, 1200 y 1400 Ma, y presentan una naturaleza peraluminosa típica de fundidos félsicos derivados de la fusión parcial cortical. Nuestros resultados respaldan modelos paleogeográficos que vinculan al CA con Oaxaquia y Gondwana occidental. Sin embargo, los datos de circones sugieren que la fuente de las poblaciones de circones detríticos y heredados podrían haber sido los terrenos metamórficos relacionados con Oaxaquia recientemente identificados en el sur de México, en lugar del tradicionalmente inferido Complejo Oaxaqueño. Adicionalmente, proponemos que la evolución metamórfica registrada durante $D_{\mathrm{LGI-2}}$ es consistente con modelos tectónicos que atribuyen esta deformación a la exhumación y el cabalgamiento de rocas de alta presión del CA sobre las RBGPP. Los nuevos datos del área de Zacatepec proporcionan información valiosa sobre la evolución de las RBGPP y los granitoides Esperanza en el CA, y podrían servir como referencia para estudios comparativos en otras áreas del complejo y para la interpretación de su evolución geológica y tectónica.

Palabras clave: metamorfismo de bajo grado; modelado de equilibrio de fases; geotermobarometría; geocronología U-Pb de circón; Complejo Acatlán; México.

INTRODUCTION

Prograde low-grade rocks are typical constituents of many metamorphic complexes around the world (Ortega-Gutiérrez, 1978; Árkai et al., 2003; Zheng et al., 2005; Baltazar and Zucchetti, 2007; Pò et al., 2016; Franceschelli et al., 2017; Balen et al., 2018; Petroccia et al., 2024), bearing key information on their geological evolution. They can act as a bridge to understand the geological history of a zone from protolith formation to metamorphic history, which highlights the importance of conducting studies that examine different aspects of their evolution. They tend to preserve primary features, such as pillow morphologies in metalavas (Ortega-Gutiérrez, 1978; Baltazar & Zucchetti, 2007) or sedimentary structures and fossils in metasedimentary rocks (Powell, 2003; Ortega-Obregon et al., 2009), while geochronometers, such as zircon, experienced low disturbance, thus preserving valuable information on the protolith history. In volcano-sedimentary sequences, the neoformation of metamorphic minerals is often contemporaneous with the development of foliations, lineations, and folds that inform about the metamorphic and deformational history of lithodemic provinces (Freeman et al., 1997; Torres Carbonell et al., 2017). However, obtaining quantitative geothermobarometric results of those deformation episodes for lowgrade rocks is often challenging due to the scarcity of appropriate geothermobarometers, the limitations that arise in thermodynamic phase modeling (such as the wide P-T range of the high-variance mineral assemblages), the inconsistencies between observed mineral compositions, the high uncertainties of the compositional models at low temperatures, and the difficulty to obtain the reactive bulk composition (e.g. Petroccia et al., 2024).

Low-grade rocks constitute the majority of the rocks outcropping in the Acatlán Complex, southern Mexico (Figure 1). Data and interpretations from these rocks have been crucial for refining the tectonic models proposed for their evolution (e.g., Keppie et al., 2008b; Ortega-Gutiérrez et al., 2018). Several works provide information on their contact relationships with other components of the complex, and the timing of the formation of their protoliths (Keppie et al., 2006, 2008b, 2008a; Ramos-Arias et al., 2008; Grodzicki et al., 2008; Hinojosa-Prieto et al., 2008; Morales-Gámez et al., 2008; Kirsch et al., 2014), their deformational history (Malone et al., 2002; Ramos-Arias et al., 2008, 2012; Grodzicki et al., 2008; Hinojosa-Prieto et al., 2008), descriptive and qualitative petrology, as well as the cooling ages of metamorphic minerals (Hinojosa-Prieto et al., 2008; Ortega-Obregón et al., 2009; Kirsch et al., 2014). Despite the increasing amount of information available for the low-grade rocks of the Acatlán Complex, it primarily focuses on the eastern, northern, and western parts of the Complex, while the central and southern portions lack detailed geological information beyond mapping (e.g., Ortega-Gutiérrez et al., 1999; Mendoza-Rosales et al., 2024). Moreover, quantitative geothermobarometry in low-grade rocks is scarce in the literature, which limits our understanding of the tectonometamorphic history of the Acatlán Complex. In the southern Acatlán Complex, around the area of San Martín Zacatepec, low-grade rocks in contact with deformed granitoids occur, but no data have been reported for them.

To address this gap, we present a characterization of the lithological units outcropping in the Zacatepec area, along with structural and deformational analysis, U-Pb zircon data for metasedimentary rocks and metagranitoids, and quantitative geothermobarometry data for

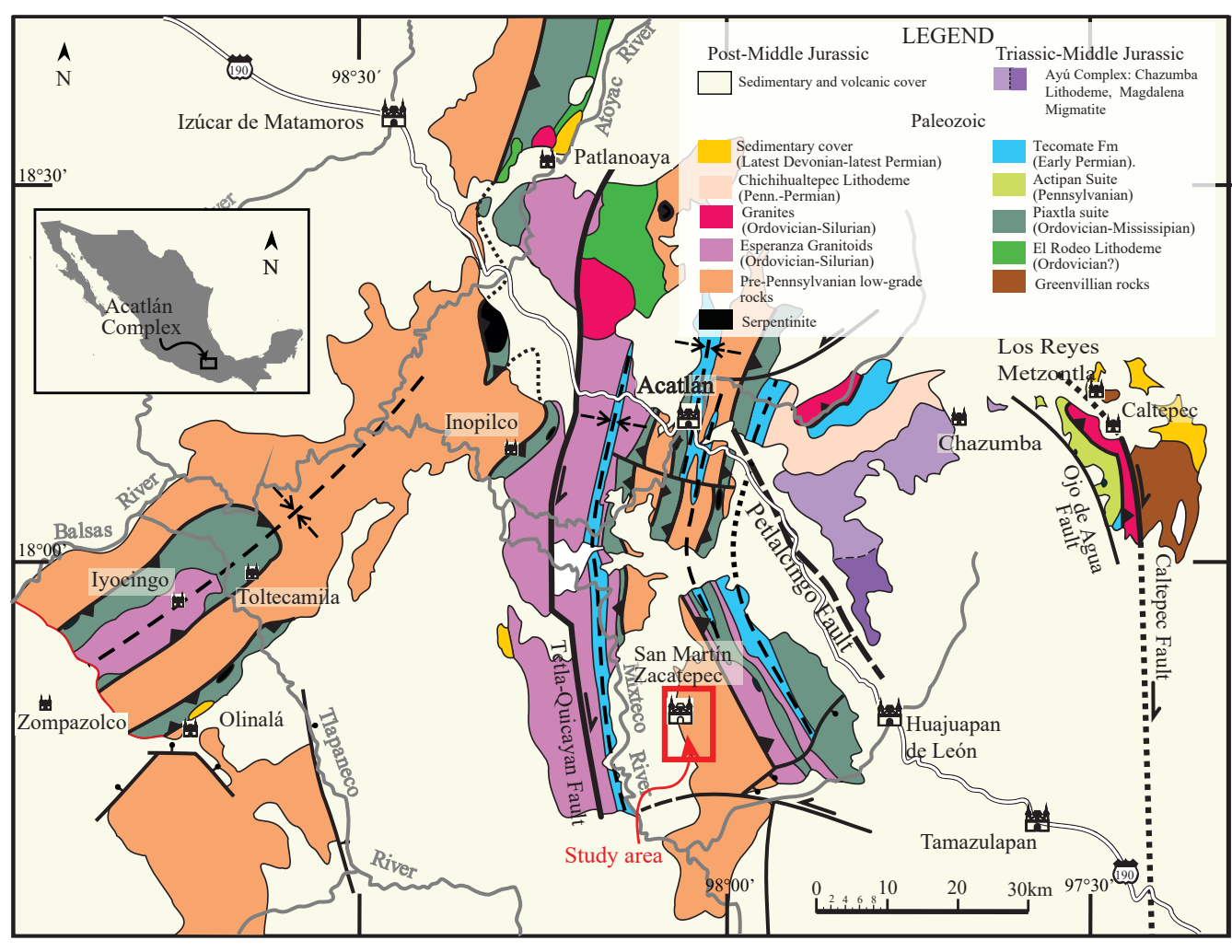


Figure 1. Regional geological map of the Acatlán Complex highlighting the location of the study area (modified from Ortega-Gutiérrez et al., 1999; 2018).

the low-grade rocks, obtained using phase equilibria modeling and classic thermometry. Our results are relevant for the evolution of the Acatlán Complex since they report new localities of lithologies correlated to other pre-Pennsylvanian low-grade rocks and the Esperanza granitoids, provide quantitative proxies for the metamorphic evolution of the pre-Pennsylvanian low-grade rocks, and open the discussion to the interpretation of the Grenvillian sources of the Acatlán Complex lithologies, which could be relevant for paleographic reconstructions.

GEOLOGICAL SETTING

The Acatlán Complex (AC; Figure 1) is a Paleozoic subduction-related metamorphic complex outcropping in southern Mexico (Ortega-Gutiérrez, 1978; Yañez et al., 1991; Ortega-Gutiérrez et al., 1999; Nance et al., 2006; Keppie et al., 2008b). This complex represents the basement of the Mixteca terrane (Campa & Coney, 1983), which is bounded to the Zapotecan terrane along the Caltepec fault (Elías-Herrera & Ortega-Gutiérrez, 2002), where Oaxaquian Grenvillian rocks and the AC are in contact. To the south, the Chacalapa fault represents the boundary with the Xolapa Complex (Tolson, 2005; Torres de León, 2005). To the east, the Mixteca terrane is in contact with the calcareous rocks of the Cretaceous Morelos platform along the Papalutla Thrust (Cerca-Martínez, 2004; Silva-Romo, 2008; Ruíz-

Arriaga, 2018). To the north, the AC is covered by the Cenozoic rocks of the Trans-Mexican Volcanic Belt (Gómez-Tuena *et al.*, 2007).

The AC (Figure 1) is mainly composed of low-grade rocks which, in most of the complex, are tectonically overlain by high-pressure (HP) rocks. Historically, the low-grade rocks were formerly known as the Cosoltepec Formation but were later subdivided into several units (Ortega-Gutiérrez et al., 2018, and references therein). The high-pressure rocks are commonly grouped in the Piaxtla suite, which comprises the Esperanza granitoids, the eclogitic and metapelitic rocks of the Xayacatlán Formation, and blueschists and serpentinitic bodies (Ortega-Gutiérrez et al., 2018 and references therein). The most recent quantitative geothermobarometry shows that the eclogites reached peak conditions at ca. 520-700 °C and 1.8-2.3 GPa (Hernández-Uribe, 2022), while the blueschist experienced peak metamorphism at ca. 505 °C and 1.9 GPa (Hernández-Uribe et al., 2019). The timing and number of events associated with high-pressure metamorphism are still debated. Some authors argue for a Late Ordovician-early Silurian high-pressure event based on monazite 418 ± 18 Ma U-Pb ages for deformed portions of the Esperanza granitoids, which overlaps with the oldest 410-380 Ma Sm-Nd garnet-whole rock ages obtained from eclogites (Yáñez et al., 1991). Other authors, in contrast, have presented garnet Lu-Hf ages for amphibolitic eclogites (352.5±1.6Ma; Estrada-Carmona et al., 2016), U-Pb zircon ages from retrograded eclogites (353 ± 1 Ma; Elías-Herrera et al., 2007), and Ar-Ar cooling ages of phengite and glaucophane from blueschists (341 Ma; Elías-Herrera *et al.*, 2007), suggesting the HP metamorphism occurred during the Mississippian.

The Tecomate Formation rests uncomfortably on both the high-pressure rocks of the Piaxtla suite and the low-grade volcano-sedimentary rocks, and was deposited during the latest Pennsylvanian to earliest Permian (Sánchez-Zavala *et al.*, 2004).

Low-grade metasedimentary units of the Acatlán Complex

Low-grade rocks comprise 70–80 % of the exposed surface of the AC (Figure 1), with most of them bearing pre-Pennsylvanian protolith ages with similar characteristics (Ortega-Gutiérrez et al., 2018). Some authors interpret them as part of a single Cosoltepec Formation/San Jerónimo assemblage (Ortega-Gutiérrez, 1978; González-Ixta, 2024), while others subdivide them into different metavolcanic-sedimentary units mainly based on their U-Pb detrital zircon geochronology (Keppie et al., 2006, 2008a; Grodzicki et al., 2008; Hinojosa-Prieto et al., 2008; Morales-Gámez et al., 2008; Ortega-Obregón et al., 2009; Kirsch et al., 2014). To avoid a formal classification and since the debate over their division is beyond the scope of this paper, we keep the names that have been assigned to them locally in previous publications. However, we refer to them collectively as pre-Pennsylvanian low-grade rocks (PPLGR) to facilitate their description and further discussion.

The PPLGR mainly consists of metasedimentary rocks intercalated with meta-volcanic lithologies and intrusive bodies (Ortega-Gutiérrez, 1978). The proportion of metasedimentary rocks varies from location to location, but they are mostly represented by chlorite- and mica-metapelites and metapsammites, with lower proportions of metagreywackes, quartzites, metarkoses, and chert layers (Ortega-Gutiérrez, 1978; Talavera-Mendoza et al., 2005; Keppie et al., 2006, 2008 a; Grodzicki et al., 2008; Hinojosa-Prieto et al., 2008; Morales-Gámez et al., 2008; Ortega-Obregón et al., 2009; Kirsch et al., 2014). Meta-volcanic rocks, including pillow lavas (Ortega-Gutiérrez, 1978; Grodzicki et al., 2008; Ortega-Obregón et al., 2009), rhyolites (Grodzicki et al., 2008; Keppie et al., 2008a), and rare ash layers (Ortega-Obregón et al., 2009) appear within the metasedimentary layers, whose contacts are interpreted as depositional.

The maximum depositional ages (MDA) of the PPLGR have been interpreted from zircon data, typically on the basis of the youngest single concordant grain or the youngest cluster of concordant grains. The interpreted MDA for the defined units consists of two main groups: (1) Mississippian-Devonian ages for the Zumpango (ca. 327 to 385 Ma, Ortega-Obregón et al., 2009), Amarillo (339 \pm 6 Ma; Kirsch et al., 2014), Salada (352 \pm 3 Ma; Morales-Gámez et al., 2008), El Naranjo (354 ± 7 Ma; Ortega-Obregón et al., 2009), Coatlaco $(357 \pm 35 \text{ Ma}; \text{Grodzicki } et \text{ al.}, 2008)$, and Progreso $(402 \pm 4 \text{ Ma};$ Ortega-Obregón et al., 2009) units; and (2) Ordovician-Cambrian ages for Las Calaveras (448 to ca. 497 Ma; Hinojosa-Prieto et al. 2008), Amate (452 ± 6 Ma; Morales-Gámez et al., 2008), Huerta (455 ± 4 Ma; Keppie et al., 2006), Canoas (459±14 Ma; Hinojosa-Prieto et al. 2008), Ojo del agua (466±25 Ma; Keppie et al., 2008a), Mal Paso (482±25 Ma; Keppie et al., 2008a), El Epazote (488±10 Ma; Hinojosa-Prieto et al. 2008); Las Minas (496±25 Ma; Keppie et al., 2008a), and Otate (post-496±25 Ma; Keppie et al., 2008a) units and El Pitayo Lithodeme (513 Ma, González-Ixta, 2024). These MDAs are further constrained by U-Pb geochronology of metagranitoids and pegmatites that crosscut the metasedimentary rocks, yielding crystallization ages of 485-447 Ma (Keppie et al., 2006; Morales-Gámez et al., 2008). Mafic dykes with rift-like and intra-plate-like compositions (Grodzicki et al., 2008; Keppie et al., 2008a; Kirsch et al., 2014) also show Ordovician crystallization ages (Keppie et al., 2008a; Ortega-Obregón et al., 2009), suggesting bimodal magmatism. Besides providing age constraints to the low-grade volcano-sedimentary sequences, the mafic and felsic dykes, along with the geological observations, indicate that the protoliths of the PPLGR of the AC were deposited in an oceanic environment associated with rifting during the opening of the Rheic Ocean (Keppie *et al.*, 2006, 2008b; Murphy *et al.*, 2006; Hinojosa-Prieto *et al.*, 2008; Grodzicki *et al.*, 2008; Morales-Gámez *et al.*, 2008; Ortega-Obregón *et al.*, 2009).

The detrital zircon U-Pb age spectra of the PPLGR show some variations. However, they commonly depict peaks around 1100 Ma and 540-560 Ma (Figure 2a) with minor peaks around 600-700 Ma and 1000 or 1200 Ma (Figure 2a). The Cambrian to Neoproterozoic ages have been typically related to Amazonia, the Brasiliano orogen, and the Maya block (Keppie et al., 2006; Morales-Gámez et al., 2008; Nance et al., 2009), while Amazonia and Laurentia have been invoked as the possible source of the reported Paleoproterozoic ages (Keppie et al., 2006; Morales-Gámez et al., 2008; Nance et al., 2009). The prevalence of 900-1200 Ma zircons has also been associated with the denudation of the Oaxacan Complex (Keppie et al., 2006, 2008b; Hinojosa-Prieto et al., 2008; Grodzicki et al., 2008; Morales-Gámez et al., 2008; Ortega-Obregón et al., 2009). The source of the Mississippian zircon grains is not well established. However, it has been suggested that they might represent an eroded arc related to the subduction of the AC (Keppie et al., 2008b), or zircons from the exposed high-pressure rocks (Grodzicki et al., 2008; Ortega-Obregón et al., 2009). The provenance analyses highlight the importance of studying low-grade rocks of the AC to understand its paleogeography and the configuration of continental masses during the formation of Pangea.

The metasedimentary rocks and the intruding dykes show signs of penetrative deformation and metamorphism. Detailed characterization of the penetrative structures revealed that the PPLGR records between three and four deformation events (Malone et al., 2002; Grodzicki et al., 2008; Hinojosa-Prieto et al., 2008; Ramos-Arias et al., 2008, 2012; Napomuceno-Eslava, 2022). Event D₁ produced a penetrative foliation (S1) that was later isoclinally folded (F2) during D2, generating a S_2 foliation parallel to S_1 and a distinct lineation (L_2), named as foliation transposition. The tight isoclinal folds of D2 generally dip N-NE. Folds of D₂ event were openly folded during D₃; some sheath folds developed during D₂ (Malone et al., 2002; Hinojosa-Prieto et al., 2008; Grodzicki et al., 2008; Ramos-Arias et al., 2008; 2012). Foliations, lineations, and folds are commonly defined by minerals such as chlorite, muscovite, and rare biotite (Malone et al., 2002; Hinojosa-Prieto et al., 2008; Grodzicki et al., 2008; Ramos-Arias et al., 2008, 2012), suggesting sub-greenschist to upper greenschist facies syntectonic metamorphism, although amphibolite facies conditions have been inferred for the Amarillo unit (Kirsch et al., 2014). González-Ixta, 2024 reported preliminary P-T conditions of 260-360 °C and 0.20-0.43 GPa for the D_{1-2} syn-tectonic metamorphism in the locality of El Pitayo Lithodeme, using chlorite thermometry and pseudosection modeling. Ar-Ar mica ages in separate grains and K-Ar in-situ ages suggest D₁₋₂ occurred in the Mississippian (328–346 Ma), and it is interpreted to be associated to the timing of high-pressure rocks extrusion and thrusting over the PPLGR (Hinojosa-Prieto et al. 2008; Ramos-Arias et al., 2008; Ortega-Obregón et al., 2009; Kirsch et al., 2014; González-Ixta, 2024), while younger Ar-Ar and K-Ar ranging from 220 to 270 Ma most likely represent the development of D₃ and might be associated to the breakup of Pangea (Hinojosa-Prieto et al. 2008; Ramos-Arias et al., 2008; Ortega-Obregón et al., 2009; Kirsch et al., 2014; González-Ixta, 2024).

The Tecomate Formation is less studied, but it is also a low-grade volcano-sedimentary unit occurring in the AC (Figure 1). It is inferred that its original relationship with other rocks of the AC is depositional. The Tecomate Formation contains pelitic schists and metapsammites,

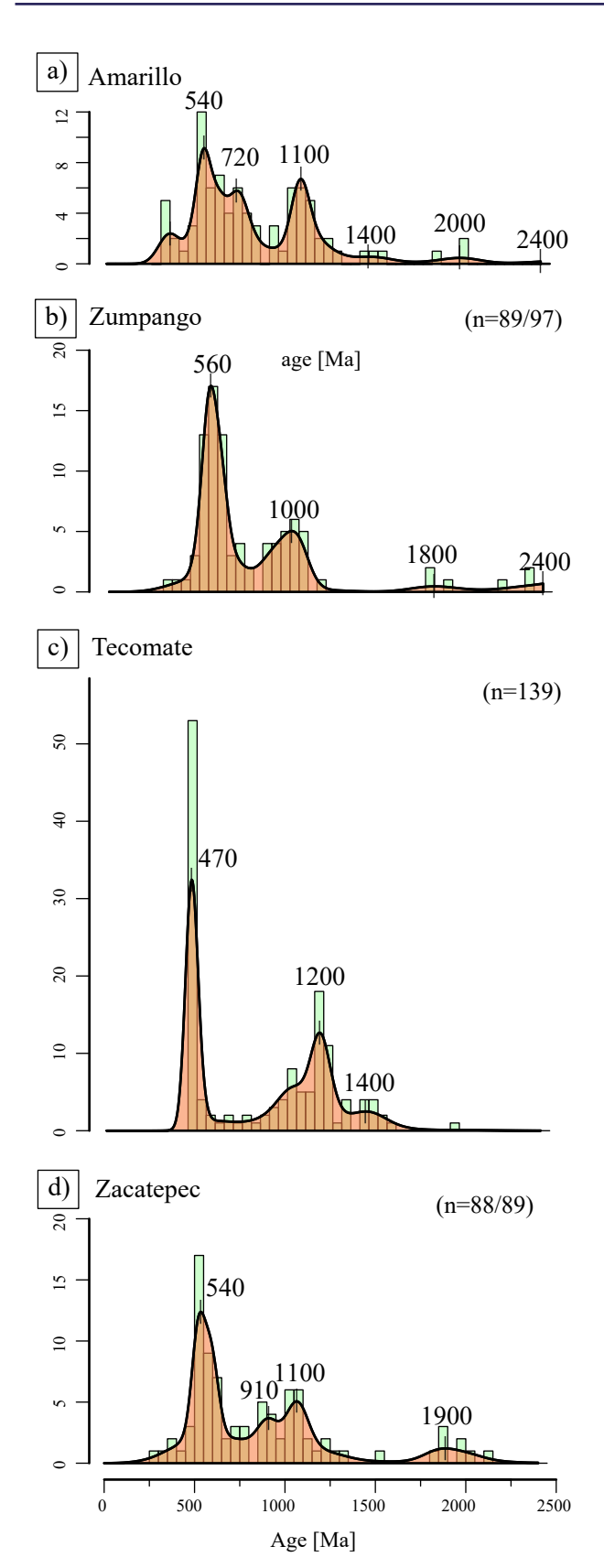


Figure 2. Kernel density estimation (KDE) plots of zircon U-Pb ages for different low-grade rocks of the Acatlán Complex (a) Amarillo unit (Kirsch et al., 2014), (b) Zumpango unit (Ortega-Obregón et al., 2009), (c) Tecomate Formation (Sánchez-Zavala et al., 2004), (d) Zacatepec metapsammite (this study).

but contrary to the PPLGR, it displays common horizons of metaconglomerate and limestone/marble lenses, which show it also was deposited in a subaqueous environment (Malone et al., 2002; Keppie et al., 2004; Sánchez-Zavala et al., 2004; Morales-Gámez et al., 2008, 2009). The Tecomate Formation shows variable deformation, but it shares the second and third interpreted deformation events recorded in the PPLGR, lacking only the earliest foliation formed during D₁ (Malone et al., 2002). Bedding is preserved in some areas, and it was folded into tight folds (Malone et al., 2002; Morales-Gámez et al., 2009), as well as upright open folds and sheath folds during D_{T1} (Morales-Gámez et al., 2009). D_{T1} also developed mineral lineations and elongation of conglomerate clasts (Malone et al., 2002; Morales-Gámez et al., 2009). The fabrics of D_{T1} were later folded by open upright NE-NW folds during D_{T1} (Malone et al., 2002; Morales-Gámez et al., 2009). These two deformation events are generally associated (Malone et al., 2002) with the Caltepec fault movement (Elías-Herrera & Ortega-Gutiérrez, 2002) during the Permian.

Detrital zircons from different rocks (Sánchez-Zavala et al., 2004) at the base of the Tecomate Formation show a dominance of ca. 470 Ma Ordovician zircons, with smaller populations of ca. 1000–1200 Ma late Mesoproterozoic zircons, ca. 1400-1500 Ma early Mesoproterozoic zircons and subordinate grains of Cambrian-Neoproterozoic ages (Figure 2c). Granitoid pebbles at the top of the formation returned *ca*. 280-320 Ma ages, which along with the discovery of latest Pennsylvanian to early middle Permian conodonts and fusilinids in marbles capping the volcano-sedimentary sequence (Keppie et al., 2004) show its deposition occurred during the latest Paleozoic, post-dating the formation of most of the AC rocks. Some similarities are observed in the zircon U-Pb age spectra of the rocks at the base of the Tecomate Formation and the PPLGR (e.g., Figure 2), and thus similar sources have been invoked to explain their age ranges. The main sources seem to be the Esperanza granitoids that have crystallization ages between 440-470 Ma (Yáñez et al., 1991; Ortega-Gutiérrez et al., 1999; Talavera-Mendoza et al., 2005; Miller et al., 2007; Vega-Granillo et al., 2007; Ramos-Arias et al., 2008), which is consistent with their proximity since the Tecomate Formation is often structurally above the granitoids in direct contact (e.g., Sánchez-Zavala et al., 2004; Mendoza-Rosales et al., 2024; Maldonado et al., 2025).

Deformed metagranitoids in the Acatlán Complex

Several metagranitoids crop out across the AC (Figure 1). They commonly exhibit strong deformation developing mylonitic fabrics with megacrystic alkali feldspar and are collectively known as Esperanza granitoids (Ortega-Gutiérrez, 1978). Contemporaneous with the deformation, some of the granitoids underwent high-pressure metamorphism, with calculated peak conditions of 680-830 °C and 1.5-1.7 GPa, followed by clockwise exhumation to greenschist facies retrograde conditions (Vega-Granillo et al., 2007; Galaz et al., 2013). The granitoids are silica-rich and peraluminous, exhibiting evolved Nd and Sr compositions (Yáñez et al., 1991; Ortega-Obregon et al., 2010). Their zircon U-Pb age spectra, which range from Mesoproterozoic to Ordovician, are interpreted to be predominantly inherited, with the youngest concordant zircons dating the timing of crystallization that commonly returns Ordovician ages (ca. 474-442 Ma; Yáñez et al., 1991; Ortega-Gutiérrez et al., 1999; Talavera-Mendoza et al., 2005; Miller et al., 2007; Vega-Granillo et al., 2007; Ramos-Arias et al., 2008), although a few Mesoproterozoic crystallization ages have also been interpreted (Yañez et al., 1991; Talavera-Mendoza et al., 2005). Within the inherited zircon, a common population age ranges from 900-1200 Ma, which along with the isotopic data, suggests that the granitoids represent partial melts derived from a source similar to the nearby Oaxacan Complex (Yáñez et al., 1991; Ortega-Obregón et al., 2010)

METHODOLOGY

We conducted fieldwork in the Zacatepec area (Figure 3), Oaxaca, to obtain structural information and to identify and describe the outcropping lithologies. We collected (Table S1 in the supplementary material) nine samples from the Esperanza granitoids unit, four from a mylonitic band, twelve from the low-grade rocks, and four from post-deformation intrusives. Most of the samples are oriented and cut parallel to the lineations and perpendicular to the foliation, allowing us to utilize their microstructures in expanding our structural analysis. We also obtained geochronological, bulk rock chemistry, and geothermobarometric information from three samples.

The map (Figure 3) was constructed using field-based observations and data, as well as satellite image analyses (Chaverria-Urrieta, 2025), and follows the general map of the Acatlán Complex presented by Ortega-Gutiérrez et al. (1999). After field observations and obtaining different control points for the contacts, an analysis was conducted using Level-2A multispectral images from the Sentinel-2 satellite, which were obtained from the Copernicus Data Space Ecosystem (https://dataspace.copernicus.eu/). The images were then processed with the software ENVI Classic v3.4. Following the parameters established by Gupta (2011), false color composites (FCC) and band ratios using Short-Wave Infrared (SWIR) bands were generated to identify lithological variations. Visible light bands were used for Feature-Oriented Principal Component Analysis (FPCA) to extract principal lineaments according to the criteria of Elsaid et al. (2014). Additionally, a Digital Elevation Model (DEM) was downloaded from the Continental Relief section of the National Institute of Geography and Statistics of México website (https://www.inegi.org.mx/temas/ relieve/continental/). This DEM was used to analyze erosion patterns and landforms following Thornbury (1969) to distinguish lithologies, lineaments, and structures. The combination of image spectral analyses and field control points was used to extrapolate and infer lithological contacts, following the principles of geological mapping.

Bulk rock geochemistry

A garnet-bearing metapelite (JC-2310) and a and a garnet-bearing granitoid (JC-2323) were selected for bulk rock major element analysis. The sample was crushed in a tungsten mortar and then dried at 110 °C for two hours before the analysis. Fused glass beads were obtained with a mix of 0.8 g of sample and 7.8 g of $\text{Li}_2\text{B}_4\text{O}_7$ and then used to acquire major element compositions by X-ray fluorescence (XRF) analysis using a Rigaku ZSX Primus II spectrometer with a rhodium X-ray source at the Laboratorio Nacional de Geoquímica y Mineralogía (LANGEM) of the Universidad Nacional Autónoma de México (UNAM). Loss on ignition (LOI) was determined by measuring the difference in weight between 1 g of dried sample and the same sample after heating at 955 °C for 1 hour.

Scanning electron microscopy and microprobe analysis

Scanning electron microscopy (SEM) analyses and imaging were carried out at Laboratorio de Microscopia Electrónica y Microanálsis, part of the Laboratorio Nacional de Geoquímica y Mineralogía (LANGEM) of the UNAM, using a scanning electron microscope Zeiss EVO MA10 with an X-ray detector Bruker XFlash 30. Energy-dispersive X-ray (EDS) analyses and backscattered electron (BSE) images were performed at a high-vacuum and 15 kV voltage.

Electron microprobe analysis (EPMA) point analyses of garnet, biotite, and muscovite in sample JC-2310 were performed at Laboratorio Universitario de Petrología (LUP) at Instituto de Geofísica of UNAM using a JEOL JXA-8900R. Instrument operating conditions for garnets are as follows: 20 kV accelerating voltage, 20 nA beam

current, and 1 μ m beam size, with an acquisition time of 30 s for most elements, except for Na and K, for which 10 s was used. For micas, the beam current was changed to 15 nA.

Phase equilibria modeling

For geothermobarometry, phase equilibria models (pseudosections) were calculated in the MnNCKFMASHTO system with the Perple_X software version 7.1.2 (Connolly, 2005, 2009) using the hp62ver.dat file from the internally consistent database of Holland and Powell (2011). The following a-X models were used for the calculations: garnet, mica, biotite, chlorite, ilmenite (White *et al.*, 2014), and feldspar (Holland *et al.*, 2022). Quartz was considered a pure phase, and fluid compositions were assumed to be pure H_2O , as no carbonates or other phases were observed, suggesting low concentrations of other volatiles. A fixed XO_2 =0.01 was used in the calculations, enough to stabilize the observed epidote in the studied rock.

For the metapelite, two pseudosections were produced (see section 5.2). The first pseudosection was modeled using the measured bulk rock composition (Supplementary Table S2), assuming most of the volatiles in the sample are derived from the micas, since we did not observe pervasive amounts of hydrated retrograde/weathering minerals or carbonates thus for the $\rm H_2O$ content, the loss of ignition value was used. For a second pseudosection, the composition of the garnet core was extracted (see section 5.2) and weighted to the volume of garnet predicted, which mainly affected the content of $\rm SiO_2$, $\rm Al_2O_3$, $\rm FeO$, MgO, MnO, and CaO.

U-Pb zircon geochronology and chemistry

We selected one metapsammite (JC-2326) and one metagranitoid (JC-2323) for zircon U-Pb geochronology and trace element chemistry. Zircons were separated using conventional methods and mounted in epoxy for cathodoluminescence analysis at Laboratorio de Catodoluminiscencia at the Instituto de Geología of UNAM.

The U-Pb and trace element zircon analyses were performed using a Resonetics M050 system equipped with an LPX 220 excimer laser and a double volume cell S-155 coupled to a plasma Thermo ICap Qc at the Laboratorio de Estudios Isotópicos (LEI) at the Instituto de Geociencias, UNAM, following the methodology described in Solari *et al.* (2010). The primary standard used was the 91500 zircon (1062.4 \pm 0.4 Ma, Wiedenbeck *et al.*, 1995), with the Plešovice zircon (337.13 \pm 0.37 Ma, Sláma *et al.*, 2008) as the secondary standard. For the zircon chemistry, the glass NIST SRM 610 was used as the standard reference material.

The geochronological data were processed using the IsoplotR software (Vermeesch, 2018). For our analysis and discussion, we use the concordia dates calculated with IsoplotR (Vermeesch, 2018), and the discordance was calculated relative to the concordia distance from the spot analyses. We refer to "concordant dates" as those dates with discordance and reverse discordance values within 10 % range. We report the errors as 2σ .

RESULTS

Lithologies, geological features and structural geology

The studied area around the San Martín Zacatepec town is dominated by low-grade rocks that are in contact with mega-crystic meta-granitoids belonging to the Esperanza granitoids (Figure 3). The contact between the units is diffuse and is marked by a mylonitic band formed along a normal fault with an NW-SE trend (Figure 3). To the south, the AC is in contact with thick limestones along a W-E

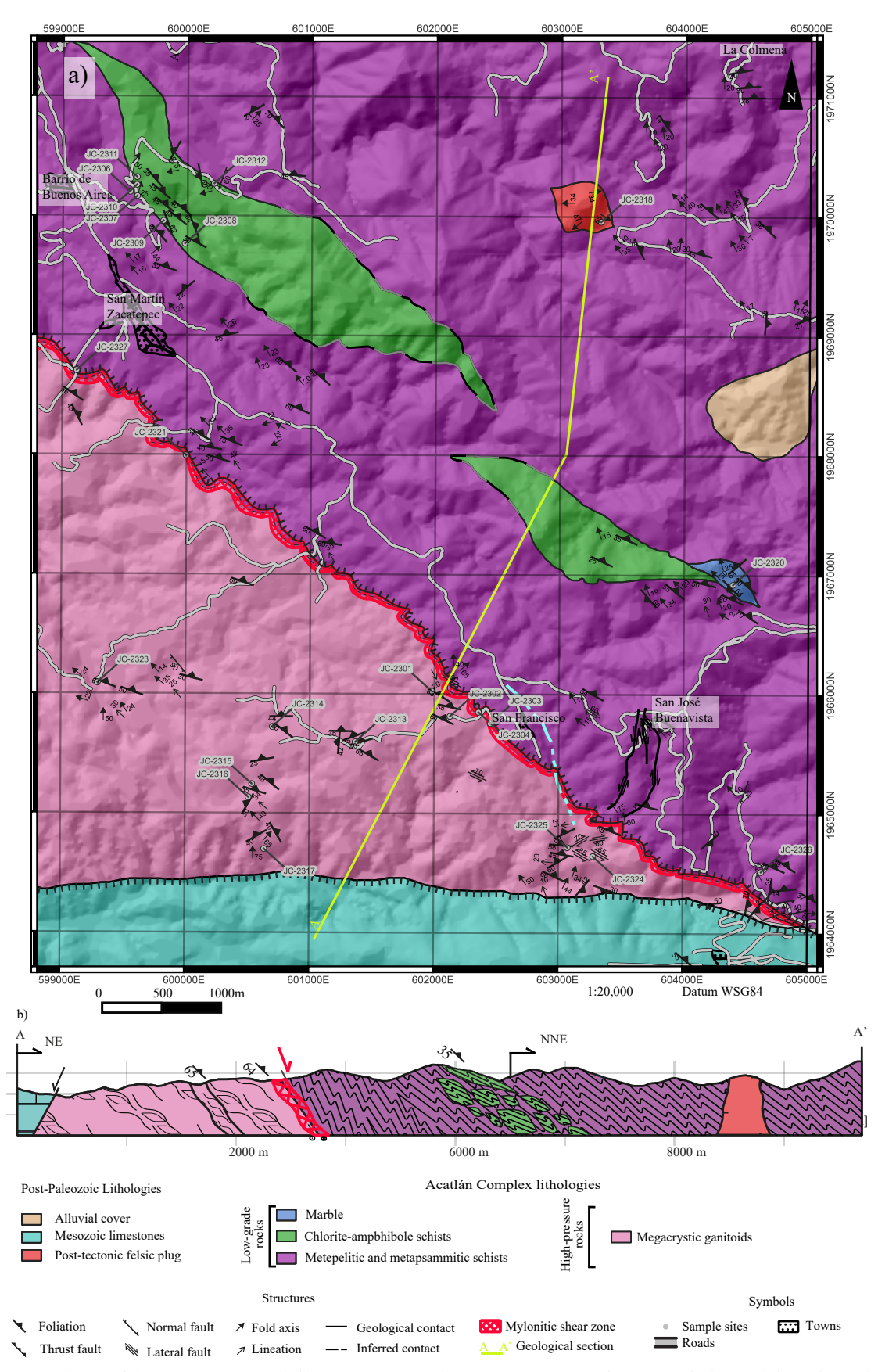


Figure 3. (a) Geological map of the Zacatepec area and (b) representative geological cross-section A-A. Constant thickness of the mylonitic band is inferred. Modified from Chaverria-Urrieta (2025).

trending normal fault (Figure 3). The metamorphic rocks in the zone are intruded by different m-sized post-deformational dykes and a *ca*. 500 m felsic subvolcanic body to the northeast (Figure 3a). Below we report the fieldwork observations and structural characteristics of the different lithologies comprising the Zacatepec low-grade rocks (ZLGR), the Esperanza granitoids in the area, the mylonitic band in their contact zone, and the intrusive bodies.

Zacatepec low-grade rocks

The ZLGR are dominantly metapsammites and metapelites (Figure 4a–4c) that mainly consist of fine to medium-grained quartz, white mica, chlorite, and opaque minerals; however, in the lower structural levels of the unit we found a *ca*. 4 m two-mica garnet-bearing metapelitic horizon (Figure 4c). In addition, soft chlorite-amphibole schists (Figure 4d) occur as m-sized horizons and as two mappable lenses

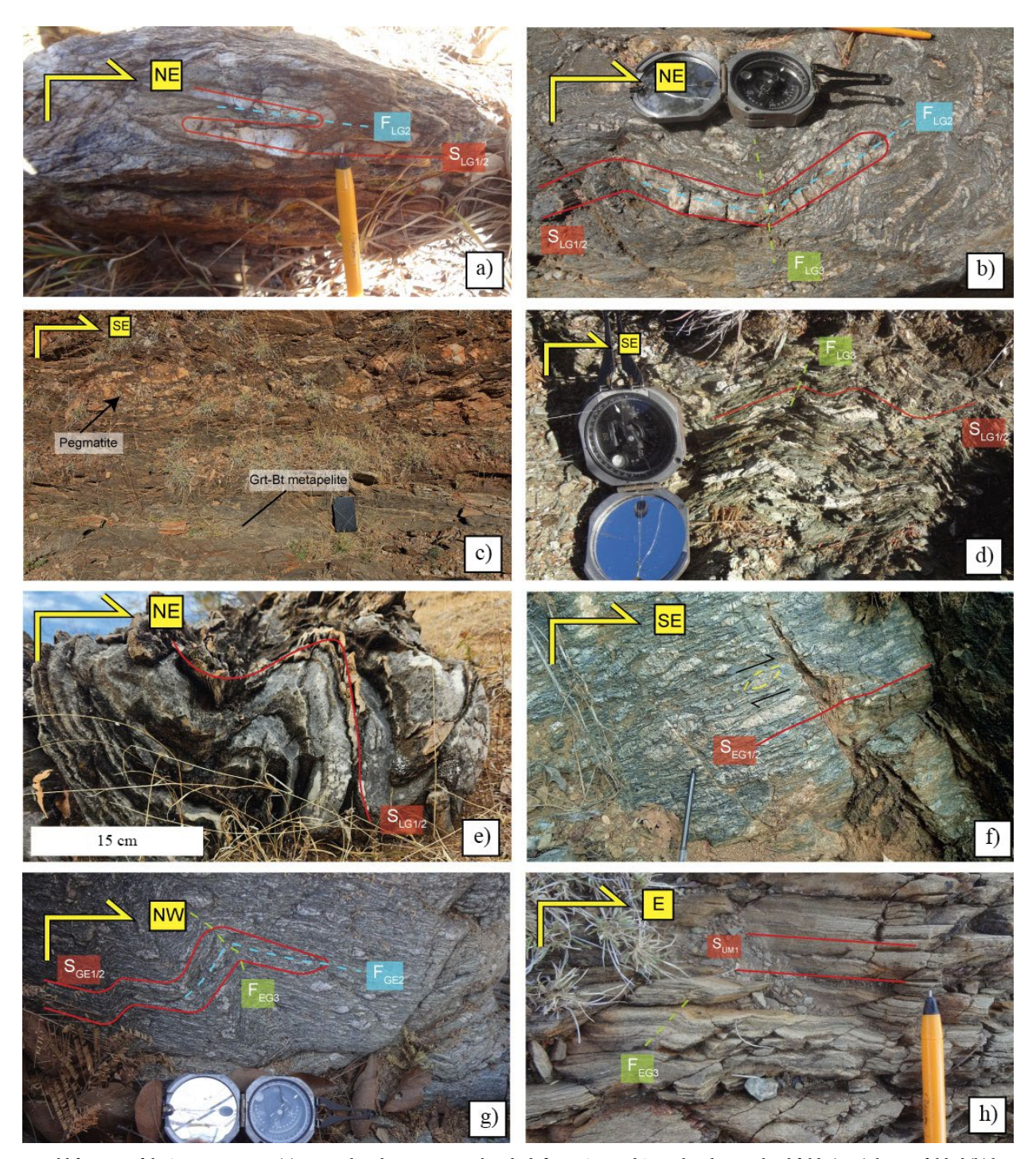


Figure 4. Field features of the Zacatepec area. (a) Metapelite showing quartz bands defining S_{LG1} and S_{LG2} related to isoclinal folds (F_{LG2}), later refolded (b) by upright open folds (F_{LG3}). (c) Metapelitic sequence with garnet-biotite schist (bottom of the photo) and intruded by a boudinaged pegmatite. (d) Amphibole-chlorite schists layers depicting $S_{LG1/2}$ affected by F_{LG3} . (e) Sheath fold in the marble. Megacrystric metagranitoids showing (f) sigmoidal structures and $S_{EG1/2}$, F_{EG2} and (g) F_{LG3} . (h) Fine layers observed in the ultramylonitic band. Foliations in red lines and fold axis in yellow dotted lines.

within the meta-sedimentary layers (Figure 3a). For the mappable chlorite-amphibole schists, we noted a gradual increase in quartz content towards the contact with the metapelites and metapsammites. A marble lens with thick calcareous layers and mm-size quartz layers also occurs in the eastern-central part of the area (Figure 3a).

All the lithologies composing the ZLGR show similar structural features (Figures 4–5). The earliest observable foliation (S_{LG1}) is defined by consistently mica schistosity and more clearly by bands of quartz (Figure 4a–4b, 5a) that are more common in metapsammites and metapelites. S_{LG1} (Figure 5b) is generally parallel to a second foliation (S_{LG2}), making their distinction difficult in most outcrops, but the quartz bands show that such foliation dips towards the SW (Figure 5a). S_{LG2} , which dips to the NNE with an average dip of 38° (Figure 5a–5d), developed due to tight isoclinal folding (F_{Z2} , Figure 4a–4b) with axes dipping at ~23° towards the NW-NNW (Figure 5a–5d). The development of F_{Z2} and S_{Z2} are contemporaneous with rare quartz lineations (L_{LG2}) dipping towards the NW. We identified another set of open upright folds (F_{LG3} ; Figure 4b, 4d) affecting F_{LG2} , whose axis dips at ~20° towards the NW. Rare sheath folds also appear in the marble layers (Figure 4e) but were not observed in other lithologies in the area.

The ZLGR are intruded along the foliation by at least one 2 m pegmatitic dykes that show a boudin structure and parallel to foliation deformation (Figure 4c). Another 1.5 m porphyric mafic dyke crosscuts the ZLGR almost parallel to foliation, it shows some >0.3 cm amphibole and plagioclase grains within a chlorite-rich matrix. The mafic dyke shows a weak foliation parallel to the foliation of the metasedimentary rocks.

To the northeast of the area, the deformation structures of the ZLGR are crosscut by a *ca*. 500 m wide tubular intrusive body (Figure 3a). The rocks of the large intrusive are felsic with a porphyritic texture and biotite phenocrysts. Magmatic flow textures and apparent magmatic isoclinal folds occur across the body. These folds are randomly oriented and show changes in the inclination of their axis, with some of them being almost vertical while others lie horizontally.

Esperanza granitoids

The Esperanza granitoids in the zone exhibit changes in grain size ranging from megacrystic (>1 cm) to fine-grained textures (<0.5 cm) both of which display mylonitic structures with some kinematic indicators (Figure 4f-4h). The megacrystic granitoids show 0.5-1 cm

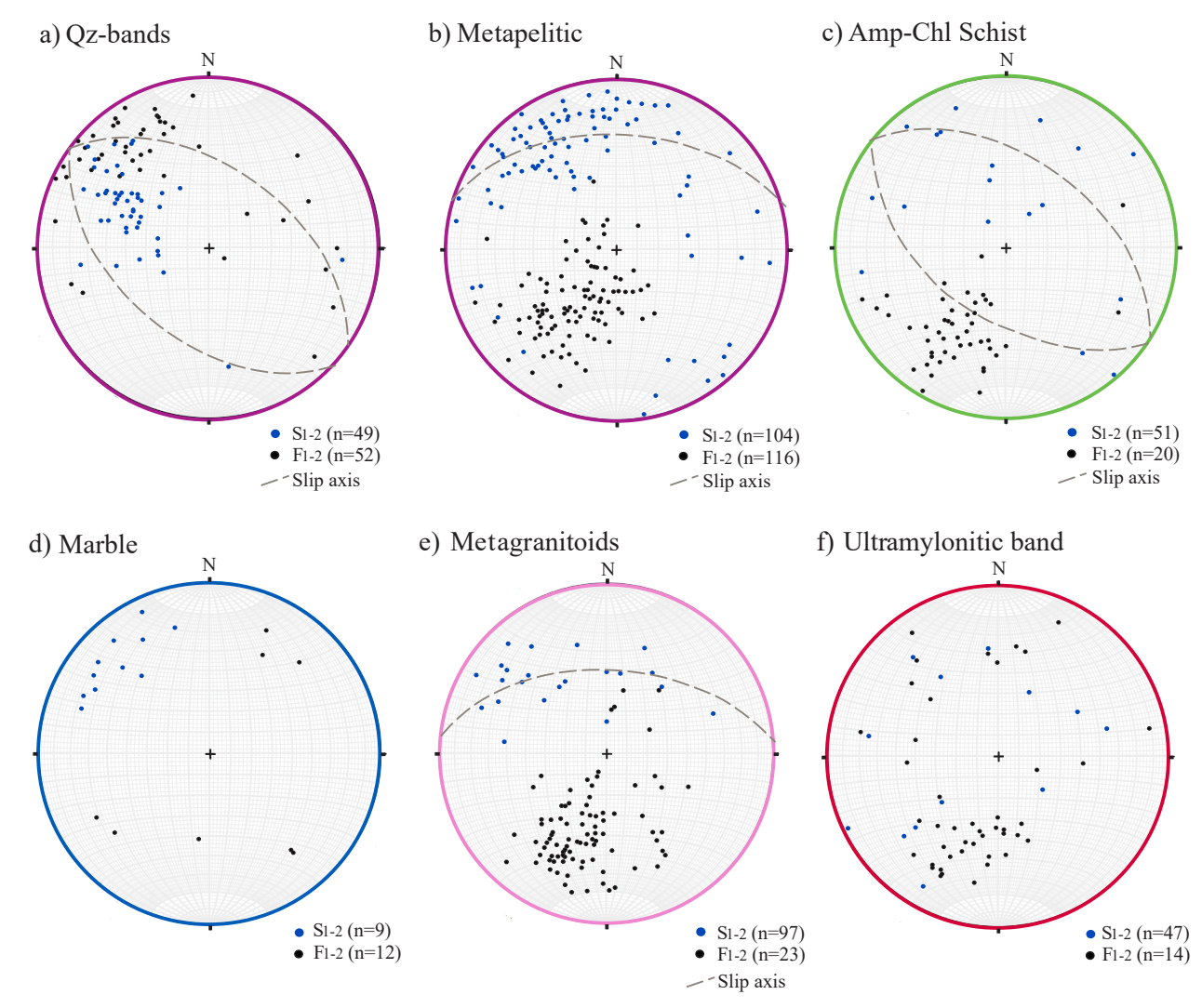


Figure 5. Representative stereograms by lithology: a) Qz bands; b) metapelitic rocks; c) Amp-Chl schist; d) marble; e) metagranitoids, and f) ultramylonitic band. Stereograms contour color as in the geological map (Figure 3). Pole to plane foliations ($S_{LGI/2}$) are ploted together with fold hinges (F_{LGI-2}). Approximate slip axis are estimated based on Hansen method. Qz: quartz; Amp-Chl: amphibole-chlorite.

bands alternating in mineralogy from quartz + chlorite + plagioclase + oxides to quartz + chlorite + white mica + garnet + rutile oxides. They present sigmoidal alkali feldspar (Figure 3f) porphyroclasts with common quartz mantles surrounding them. The fine-grained granitoids display 2–5 mm bands defined by quartz + chlorite + plagioclase grains.

The granitoids bands define the earliest foliation observable in the rocks (S_{EG1}), dipping towards the N20°E (Figure 4e, 5e), and that contains a lineation (L_{EG1}) that plunges ~30° to the NEE-NNE. Sigmoidal features parallel to the lineation found in the field show that L_{EG1} is verging towards the SE (Figure 5e). Isoclinal folds (F_{EG2}) affect S_{EG1} , developing a second foliation (S_{EG2}) parallel to S_{EG1} . Due to parallelism, the distinction between S_{EG1} and S_{EG2} is difficult in most locations. F_{EG2} is folded by cm-sized upright open folds (F_{EG3}) with an axis plunging to the NW-NE (Figure 4g).

A few intermediate porphyritic dykes, showing magmatic flow defined by plagioclase phenocrysts, crosscut the foliations and folds of the granitoids.

Ultramylonitic band

The ultramylonitic band (*ca.* 50 m in thickness) in the contact zone between the Esperanza granitoids and the ZLGR is not a separate lithology but rather a normal fault producing a sheared band of ultramylonites most likely involving both units, which are difficult to distinguish due to the fine grain and strong deformation (Figure 4h). Because of the distinct characteristics of the ultramylonite, we briefly report their features in this separate section. The ultramylonites show 2–5 mm layers composed of quartz + chlorite + opaques and layers with white mica + quartz + plagioclase + opaques.

The ultramylonites show a strong foliation (S_{UM1}) dipping ~45° to the N15°E (Figure 5f), which is affected by NNE-plunging isoclinal folds (F_{UM2}), creating a second foliation (S_{UM2}), that is also indistinguishable from S_{UM1} as is common in the area with an incipient development of S-C structures. Late open folds (F_{UM3}) affect the earlier foliations, and all are overprinted by a lineation (L_{UM3}) dipping to the NW.

Petrography

The thin-section observations provide a more detailed characterization of the metamorphic evolution of the rocks in the area. As most of them are oriented rocks, we use the kinematic indicators to provide further insights into the vergence of the deformation during the development of the $S_{LG1/2}$ and $S_{EG1/2}$ foliations. Here we present the summary of the petrographic characteristics of the samples (Supplementary Table S1), describing in more detail the mineralogy and microstructures of the garnet-bearing metapelite (JC-2310) that we used for thermobarometry using phase equilibria modeling, garnet-biotite, and Ti-in-biotite thermometry.

Zacatepec low-grade rocks

The metapelites commonly show a muscovite + biotite + quartz + chlorite + opaque mineral assemblage. Both muscovite and biotite defining the main foliation; biotite grains are overprinted by chlorite in their rims. They display different kinematic indicators, such as sigmoidal quartz and mica aggregates or isoclinal folds (Figure 6a), indicating verging towards the SE.

Within the metapelites, one sample (JC-2310) presents garnet porphyroblasts. JC-2310 is a fine grained (<100 μm) foliated rock with larger garnet porphyroblasts ranging in size from 500–1500 μm (Figure 6b). Quartz-rich bands and mica-rich bands occur within the sample and incipient S-C foliations are visible. Foliation is defined by muscovite and biotite (Figure 6b). Biotite occurs mainly as patches

on the fringes of larger muscovite grains or as thin bands defining the S' structures. Garnets are poikiloblastic with <20 μm epidote and titanite, and rare zircon and monazite inclusions (Figure 6c) defining a spiral-like internal foliation that is generally oblique to $S_{LG1/2}$ and that continues towards that external foliation (Figure 6b), indicating the inclusions and the porphyroblasts are contemporaneous to the development of S_{LG1/2}. This spiral-like internal foliation in the garnet also suggests a top-to-the-SE kinematics (Figure 6b). The external foliation tends to get deflected around garnet porphyroblasts, although some smaller grains with less inclusions overprint the foliation, suggesting some of the garnet grew late to the foliation. Epidote and titanite also occur as <20 µm grains following the foliation. These microstructural characteristics indicate garnet and biotite are syn- to late syn-tectonic, suggesting a prograde evolution for the rock. Peak mineral assemblage for sample JC-2310 comprises quartz + muscovite + garnet + biotite + epidote + titanite with accessory zircons, apatite and monazite.

The metapsammites show an assemblage comprising quartz + muscovite + chlorite + plagioclase + zircon + tourmaline + opaque. They generally show alternating fine-grained (<500 μm) and coarsegrained (>1 mm) bands dominated by quartz that are typically separated by fine-grained micas. Some sigmoidal polycrystalline quartz aggregates occur in the vicinity of the bands, showing a top-to-SE transport.

The chlorite-amphibole schists show different mineral assemblages that apparently correlate with their proximity to the metapsammites and metapelites. The schists farther from the contact typically show distinct mineralogy composed of tremolite + actinolite ± chlorite ± titanite ± opaques (Figure 6d). They show a strong foliation defined by fine-grained actinolite, tremolite, and chlorite, that wraps around actinolite sigmoidal porphyroclasts showing a top-to-SE transport (Figure 6d). Titanite and opaque minerals occur both as inclusions in the actinolite porphyroclasts and as medium-sized grains. Towards the contact with the metasedimentary rocks, the chloriteamphibole schists have the mineral assemblage actinolite + chlorite + quartz + calcite + epidote. Epidote tends to occur as medium-sized grains overprinting the foliated minerals, and closer to the transition, plagioclase, quartz, and calcite appear in larger proportions. Some fine-grained sigmoidal quartz aggregates occur in the quartz-rich zones and show a top-to-SE transport.

The marbles present a simple mineralogy composed of calcite + quartz + plagioclase (Figure 6e). They display a banded microstructure mostly dominated by mm-sized bands of calcite with granoblastic texture and thin (<250 μ m) bands of plagioclase and quartz (Figure 6e). Tourmaline appears as rare inclusions in plagioclase.

The mafic dyke crosscutting the ZLGR parallel to the foliation shows a mineral assemblage of quartz + hornblende + epidote + clinozoiste + chlorite + opaques with a dominant granoblastic microstructure with relic hornblende magmatic phenocrysts that are overprinted by chlorite and epidote towards the rims. The large felsic intrusive towards the north shows a porphyric texture with biotite phenocrysts and microcrystic plagioclase grains in the matrix.

Esperanza granitoids

The fine grained and megacrystic granitoids present slight differences in their mineralogy and microstructures, which we describe here. The fine grained granitoids display a diverse mineral assemblage containing quartz + plagioclase + phengite + chlorite + epidote \pm clinozoisite \pm allanite \pm garnet \pm zircon \pm rutile \pm tourmaline \pm opaques. Some portions are richer in mica while others are in epidote. They show a microstructure developing incipient C-C' foliations, with a top-to-ESE transport, which is consistent with mica

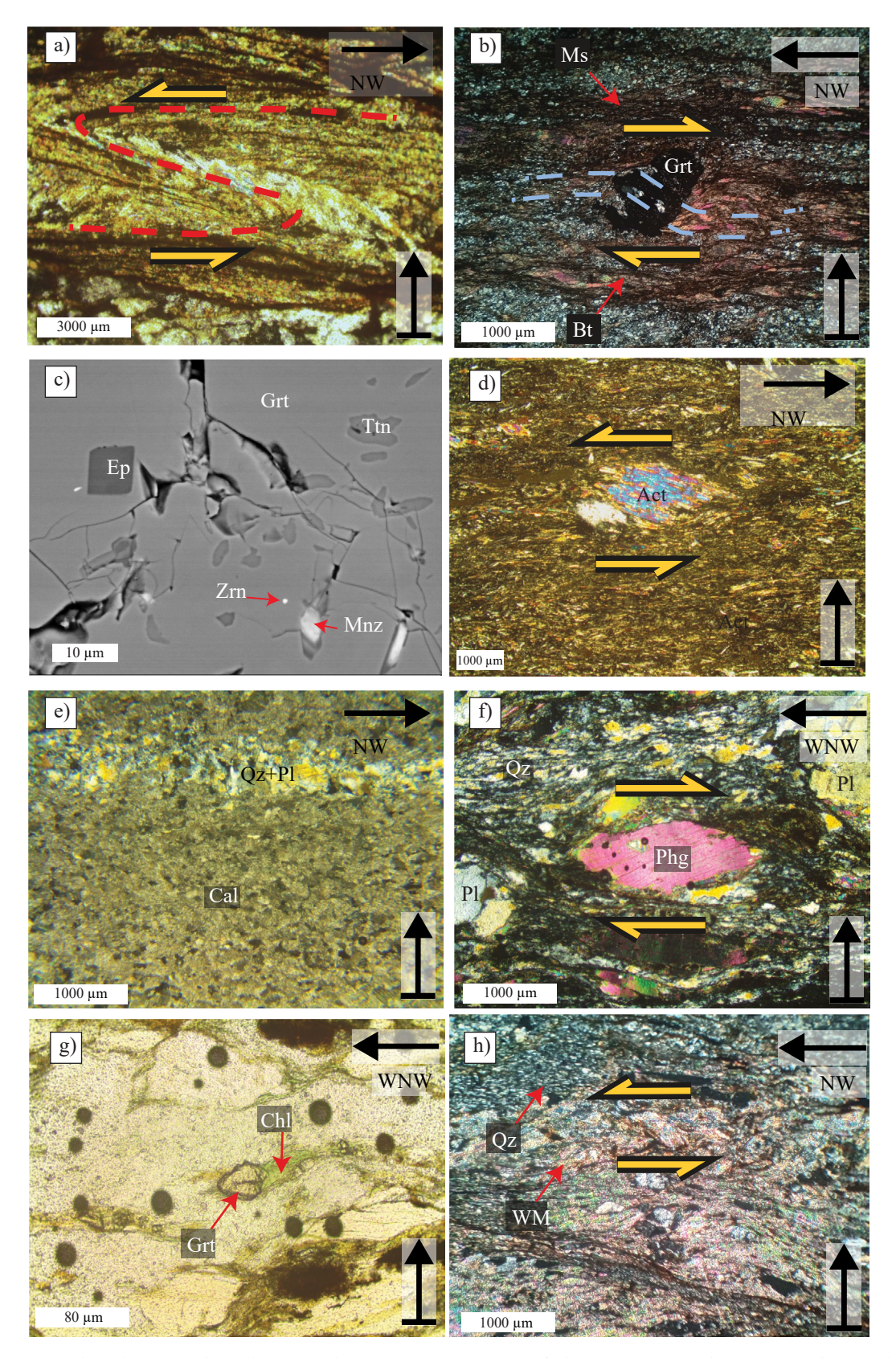


Figure 6. Photomicrographs with petrographic and scanning electron microscope. (a) Microfolds in a metapelite with SE vergence. (b) Spiral-like syn-tectonic garnet within a biotite-quartz-muscovite matrix showing a top-to-SE transport. (c) Back-scattered electron image of inclusions in garnet core in the biotite-garnet metapelite. (d) Sigmoidal actinolite porphyroblasts with top-to-SE transport. (e) Calcite and quartz-plagioclase layers in marble. (f) Sigmoidal mica fish in metagranitoid with an ESE vergence. (g) Prograde garnet in metagranitoids. (h) Mica fish showing top-to-NW transport in ultramylonite; WM: white mica. Mineral abbreviations after Whitney and Evans (2010).

fish (Figure 6f) and sigmoidal magmatic plagioclase porphyroclasts, the latter presenting a poikilitic microstructure with randomly arranged inclusions of epidote with allanite-chlorite rims. Rutile and garnet (Figure 6f) occur, but the lack of inclusions hinders their proper interpretations as syn- or pre-tectonic grains. Garnet is overprinted by chlorite and epidote (Figure 6f)

The mineral assemblage of the megacrystic portions contains quartz + microcline + biotite + phengite + chlorite \pm plagioclase. Interpreted magmatic feldspars occur as 0.5–1 cm porphyroclasts with rare quartz mantles displaying sigmoidal morphologies with a SE vergence. Late chlorite and epidote occur in the samples.

Ultramylonitic band

As observed in the field, the ultramylonitized rocks occurring along the normal fault bounding the ZLGR and the Esperanza granitoids are either characterized by a greater percentage of quartz or are dominated by micas. The mineralogy of the quartz-rich ultramylonites consists of quartz + muscovite + chlorite + opaques, while the mica-rich portions contain muscovite + quartz + plagioclase + chlorite + opaques. They present penetrative foliations and mica fish or rounded porphyroclasts indicating top-to-NW vergence (Figure 6h).

Mineral and bulk rock chemistry

We obtained bulk rock (Supplementary Table S2) and mineral chemistry (Supplementary Tables S3–S5) for garnet-bearing granitoid JC-2323 and garnet-bearing metapelite JC-2310. The garnet-bearing metapelite is a relative SiO₂-poor (54.95 wt. %) and Al₂O₃-rich (17.54 wt.%) rock with a concentration of 10.06 wt.% of FeO_{tot}, 6.89 wt.% for K₂O, 3.68 wt.% for MgO and ≤ 1 wt.% for the rest of the major elements. The garnet-bearing metagranitoid is relatively rich in SiO₂ (65 wt.%) and Al₂O₃ (14.78 wt.%) with a concentration of 6.60 wt.% of FeO_{tot}, 3.19 wt.% for K2O, 2.76 wt.% for Na2O and ≤ 2 wt.% for the rest of the major elements. The metagranitoid is a peraluminous rock with an Al/(Ca+K+Na) index =1.51.

Garnets in the metapelite (Supplementary Table S3) are spessartine-rich (X_{Sps} =0.45–0.55) crystals with similar proportions of almandine (X_{Alm} =0.20–0.28) and grossular (X_{Grs} =0.21–0.31) and

negligible contents of pyrope (X_{Prp} =0.005–0.01). Compositional transects made along two crystals (Figure 7) reveal that spessartine contents decrease from core to rim, while almandine and pyrope slightly increase and grossular composition mostly stays constant. Biotite in the metapelite shows TiO_2 contents ranging from 1.02–1.55 wt.% and Mg# (Mg/(Mg+Fe)) ranging from 0.43–0.48 (Supplementary Table S4). Muscovite in the sample shows SiO_2 concentration of 46.65–51.73 wt.% and Mg# ranging from 0.49–0.61 (Supplementary Table S5).

Geothermobarometry

To constrain the pressure and temperature conditions during the prograde metamorphism that developed the earliest foliations ($S_{\rm LG1-2}$), we applied different methods to the garnet-bearing two-mica metapelite. We calculated temperatures using the garnet-biotite thermometer (Perchuk and Lavrent'eva, 1983) for four garnet-biotite pairs in direct contact with each other. Temperatures obtained at 0.3 to 0.4 GPa range from 391 to 404 °C. We also applied the Ti-in-biotite geothermometer (Henry *et al.*, 2005) to biotite crystals and obtained variable results ranging from 430–555 °C, with a mean value of 512 °C.

To further define the metamorphic conditions and obtain quantitative pressure results, we produced pseudosections for metapelite JC-2310 (Figure 8a). Peak assemblage quartz + muscovite + biotite + garnet + epidote + titanite is stable in a small field ranging from ca. 490 to 510 °C ca. 0.47 ca. to 0.55 GPa (Figure 8a). Isopleths for TiO₂ wt.% in biotite overlap with the field, and also the isopleths for the lowest concentrations of SiO₂ in muscovite (Figure 8b). Composition of the garnet is well-reproduced with this model. The isopleths for garnet compositions from core to rim all overlap, defining a small P-T region ranging from ca. 420 to 450 °C 0.19 to 0.27 GPa (Figure 8a–8b).

Zircon geochronology and trace element chemistry

We selected one metapsammite (JC-2326) and one metagranitoid (JC-2323) to inspect them under cathodoluminescence (Figure 9a–9b) for U-Pb zircon geochronology (Figure 9c–9d) and zircon chemistry (Figure 9e–9f).

Zircons of the metapelite are mostly rounded, elongated grains showing different textures under cathodoluminescence. They

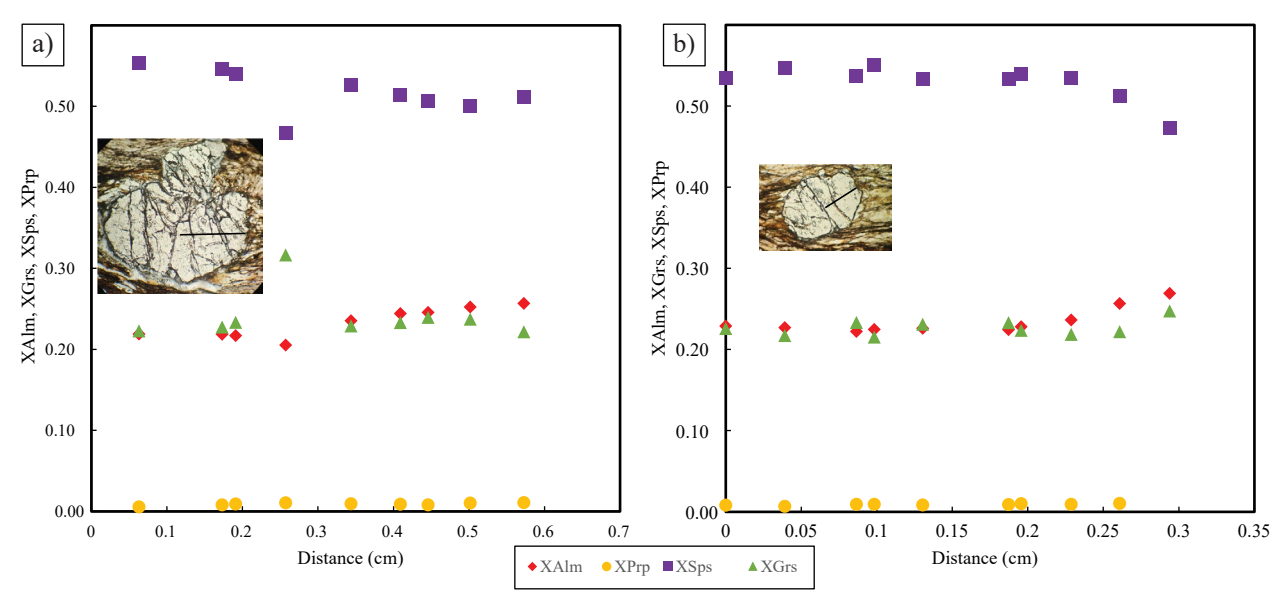


Figure 7. Garnet compositional transects for two grains (insets in figure a and b) from the garnet-biotite metapelite. Alm: almandine; Grs: grossular; Sps: spessartine; Prp: pyrope.

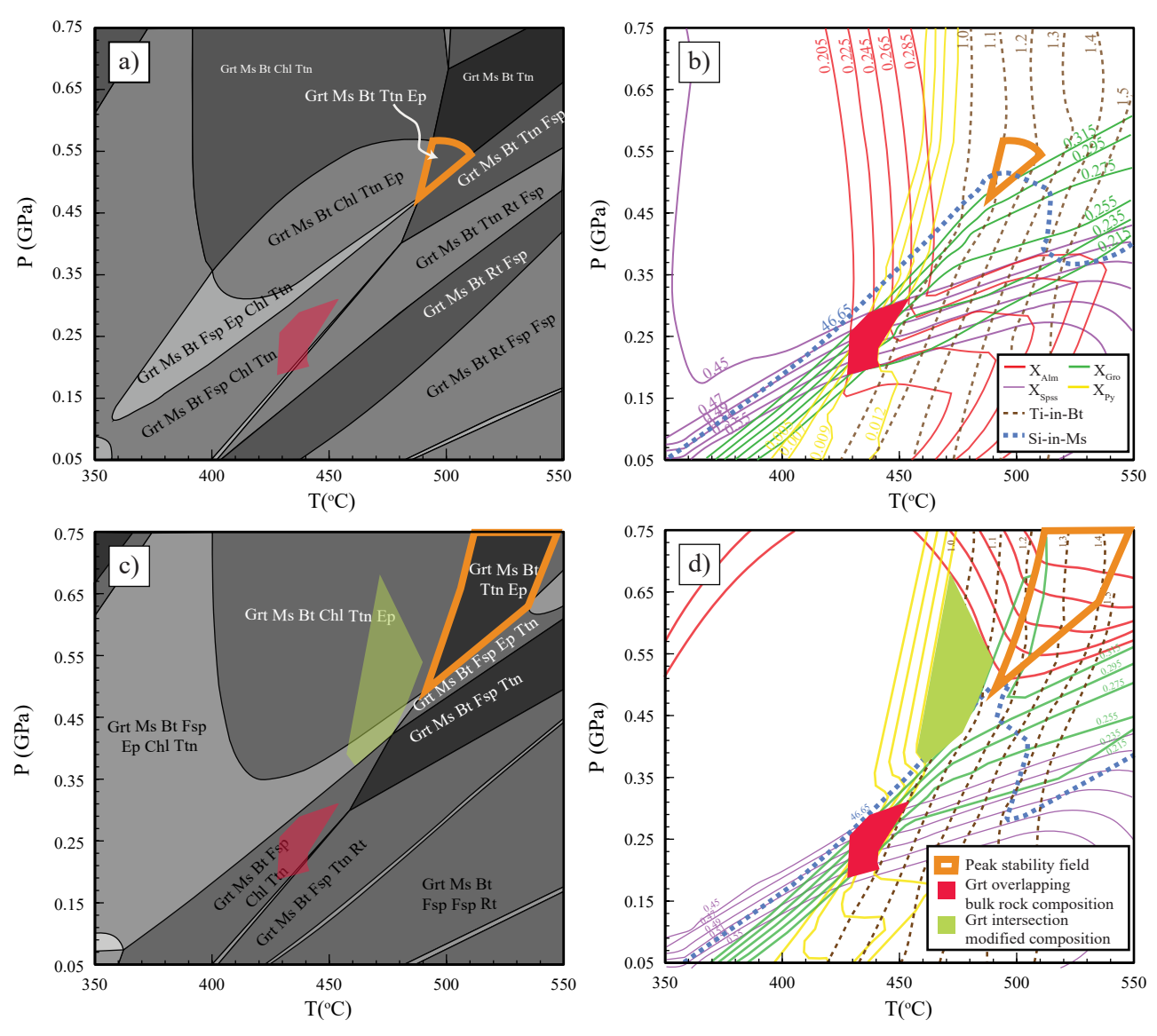


Figure 8. Phase equilibria models in the MnNCKFMASTHO system for the garnet-biotite metapelite obtained with Perplex_X (Conolly, 2005; 2009). (a) Pseudosection and (b) garnet, biotite and muscovite compositional isopleths obtained with the bulk-rock composition. (c) Pseudosection and (d) garnet, biotite and muscovite compositional isopleths obtained with the composition after garnet core extraction. Arrow in (c) represents the interpreted P-T evolution; numbers in the isopleths correspond to the measured compositions. Mineral abbreviations after Whitney and Evans (2010).

display homogenous cores or weak to well-developed oscillatory zoning (Figure 9a) and rare patchy zoning. Most of the grains do not show any visible metamorphic overgrowths. Out of the 99 analyzed zircon grains in the sample, 89 of them display a <10% discordance (Supplementary Table S6). The concordant grains range from 334 ± 8.9 to 2020.9 ± 37.2 Ma (Figure 9c). The three youngest grains are concordant, yielding Devonian to Mississippian dates of $334 \pm 8.9 \text{ Ma}$ (0.72% discordant), $378.5 \pm 8.8 \text{ Ma}$ (0.43% discordant), and 397.2 \pm 9.4 Ma (-0.93% discordant). The rest of the grains are pre-Devonian and define a younger population ranging from ca. 411 to 650 Ma, with a peak around and ca. 540 Ma, another population in the range 800-1200 Ma, with peaks around 910 Ma and 1100 Ma, and a smaller population ranging from 1810 to 2020 Ma with a peak around 1900 Ma (Figure 2d). Only two grains with 990-1020 Ma ages occur in the sample. Zircons show a general Eu negative anomaly, and higher contents of HREE than LREE (Figure 9e), except for seven

grains with dates ranging from *ca.* 519–579 Ma that display a clear HREE flat pattern (Figure 9e)

Zircons of the metagranitoid are slightly rounded, elongated grains with homogeneous, and weak oscillatory zoning, with some grains showing inherited cores (Figure 9b); a few grains show thin (<20 μm) rims. Out of the 29 analyzed zircon grains, 24 of them show discordance <10% (Supplementary Table S6). The concordant grains range from 473.6 \pm 9.6 to 1487.5 \pm 20 Ma (Figure 9d). Only one grain yields a 473.6 \pm 9.6 Ordovician date (9.9% discordant), and the next youngest grain has a 6.7% discordance and yields a 645 \pm 12.5 Ma date; the rest of the grains have dates >817 Ma. The zircon dates display a population ranging from ca.1000-1300 Ma, with two close peaks at 1100 and 1200 Ma, and another population with peak centered around 1400 Ma (Figure 10a). The zircons show negative Eu anomalies and higher contents of HREE than LREE (Figure 9f).

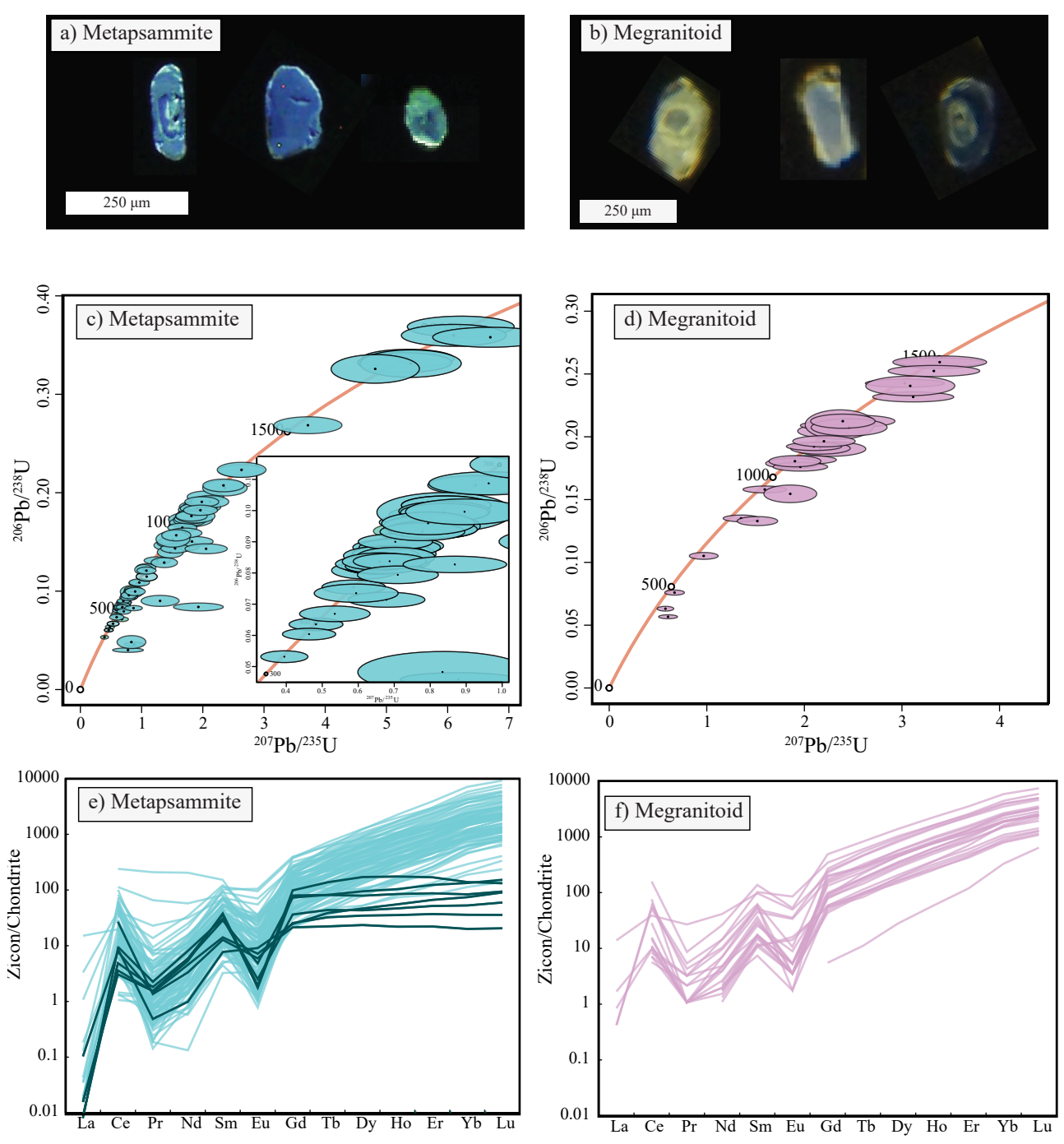


Figure 9. Zircon data for the metapsammite JC-2326 (a, c, e) and metagranitoid JC-2323 (b,d,f). (a-b) cathodoluminescence images of representative zircons; (c-d) U-Pb concordia diagrams for each sample (inset in c highlights the <700 Ma zircons); (e-f) Zircon trace element chemistry diagrams normalized to chondrite (McDonough & Sun, 1995) (patterns highlighted in e display ages between *ca*. 519-579 Ma).

DISCUSSION

General geological evolution of the Zacatepec area and correlation with other regions of the Acatlán Complex

The data collected in the Zacatepec area provide insights into the evolution of two contrasting lithological units. We will first present the description and our interpretations of the general evolution of the rocks outcropping in the area and then use this as a framework to better interpret and correlate the Zacatepec low-grade rocks (ZLGR) with other low-grade rocks across the Acatlán Complex (AC).

In the Zacatepec area, the lowest structural unit of the metamorphic rocks is represented by deformed metagranitoids, which present a peraluminous nature as shown by the high Al/(Ca+K+Na) index = 1.51 and the presence of Al-rich minerals such as phengite (Figure 6f), garnet (Figure 6g), plagioclase, and epidote. They also exhibit a diverse zircon population (473–1487 Ma; Figure 10), most of which is interpreted as inherited. These characteristics, along with the deformation, are common to the Esperanza granitoids; thus, we interpret that they belong to this larger suite outcropping along the AC (Figure 1). The peraluminous nature and the presence of inherited zircon

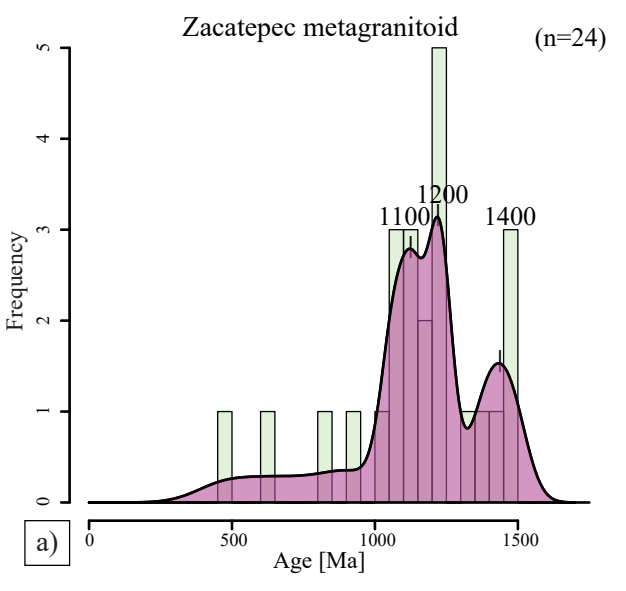
suggest the metagranitoids in the Zacatepec area are most likely the product of partial melting of an older crust, an origin common to most studied Esperanza granitoids (Sánchez-Zavala et al., 2004; Talavera-Mendoza et al., 2005; Miller et al., 2007; Ramos-Arias et al., 2008). The partial melting event that produced the Esperanza granitoids occurred during the Ordovician, as indicated by the youngest and/or largest zircon populations reported for the granitoids in other areas (Yáñez et al., 1991; Ortega-Gutiérrez et al., 1999; Talavera-Mendoza et al., 2005; Miller et al., 2007; Vega-Granillo et al., 2007; Ramos-Arias et al., 2008). However, a few granitoids bear Mesoproterozoic zircons as their youngest crystals, which has been interpreted as the age of crystallization by some authors (Yañez et al., 1991; Talavera-Mendoza et al., 2005), despite such values (e.g., 1165-1043 Ma; c.f. Talavera-Mendoza et al., 2005) overlap with the most common ranges of inherited zircons of the Esperanza granitoids (Figure 10). Here, we point out that caution must be taken when the youngest zircon grains in a granitoid with inherited zircons is interpreted as representative of the timing of crystallization, since in Zr-undersaturated magmas all the zircons may be inherited grains (c.f. Olierook et al., 2020). We therefore suggest that all the studied deformed Esperanza granitoids in the AC crystallized during the Ordovician partial melting event. We include in this interpretation our metagranitoid, since the inherited zircon age distribution in our sample is similar to that reported for the Esperanza granitoids elsewhere (Figure 10). This interpretation is corroborated, albeit weakly, by the single almost discordant (9.9% discordance) Ordovician value (473. 6 ± 9.6 Ma) that we found in the garnet-bearing granitoid of the Zacatepec area.

The Esperanza granitoids in the Zacatepec area experienced three deformation events. The first event $D_{\rm EG1}$ developed the $S_{\rm EG1}$ foliations that were later affected by $D_{\rm EG2}$ which developed rare isoclinal tight $F_{\rm EG2}$ folds and a second $S_{\rm EG2}$ foliation parallel to $S_{\rm EG1}$ (Figure 4f–4g); these fabrics are contemporaneous with phengite (Figure 6f), rutile, and probably garnet (Figure 6g), indicating high-pressure conditions. Kinematic indicators (Figure 4f, 6f) suggest top-to-SE transport during $D_{\rm EG2}$. The earlier fabrics were later affected by a third deformation event ($D_{\rm EG3}$) that developed upright cm-sized open folds ($F_{\rm EG3}$; Figure 4g). Retrograde chlorite affects the granitoid, but no clear association with the (micro)structures was observed.

The Esperanza granitoid here is directly overlain by the ZLGR along a normal fault that developed a mylonitic band that affected both units (Figure 3, 4i). We argue that this fault post-dates the deformation both of the ZLGR and the metagranitoid because of the observed grain size reduction in both of them, the NW-SE orientation of the fault that follows the foliations, and the rare opposite top-to-NE kinematic indicators occurring only within the band.

The ZLGR are predominantly composed of metapelites and metapsammites, with intercalated <1000 m chlorite-amphibole schists and marble lenses (Figure 3). Although a deeper analysis of the protolith of the chlorite-amphibole schists is beyond the scope of this paper, we suggest that they represent metamorphosed silica-poor metaigneous rocks deposited within a metasedimentary sequence. This interpretation is supported by the transitional change to higher quartz contents towards the contacts with the siliciclastic rocks and their occurrence as sparse, thin layers across the entire Zacatepec area. The sediments were probably deposited in a sub-aquatic environment, as suggested by the presence of marble lenses. For the maximum deposition age (MDA) we considered the youngest concordant zircon U-Pb analysis of the metapsammite JC-2326, which returned a Mississippian age of 334 ± 8.9 Ma.

After their deposition, the ZLGR experienced three discrete deformation events. D_{LG1} produced the NE-dipping S_{LG1} foliations (Figure 5a–5d), which were later isoclinally folded (F_{LG2}) during



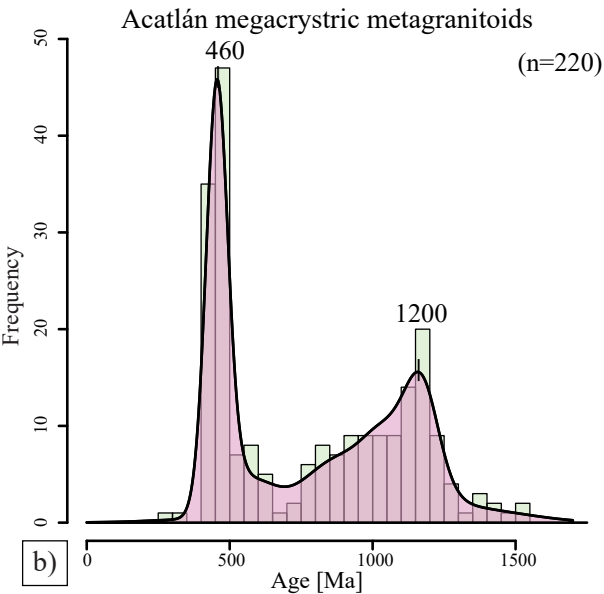


Figure 10. Kernel density estimation (KDE) plots of U-Pb ages for (a) the zircons obtained for the metagranitoids JC-2323 and (b) zircons reported for the Esperanza granitoids (Yañez *et al.*, 1991; Sánchez-Zavala *et al.*, 2004; Talavera-Mendoza *et al.*, 2005; Miller *et al.*, 2007).

 D_{LG2} , developing a second S_{LG2} foliation parallel to S_{LG1} (Figure 4a), which makes the distinction between these two foliations difficult. D_{LG1-2} fabrics are the most penetrative of the region and were contemporaneous to metamorphism that produced minerals like chlorite (Figure 6a), muscovite (Figure 6a–6b), amphiboles (Figure 6d), biotite (Figure 6b), epidote (Figure 6c) and rare syn-tectonic spiral-like garnets (Figure 6b). Kinematic indicators (*e.g.*, Figure 6a–6b, 6d) show that the ZLGR experienced top-to-SE transport during D_{LG1-2} . The ZLGR were later affected by a third, less pervasive deformation event D_{LG3} , that created upright mm- to cm-sized open folds (F_{LG3} , Figure 4b, 4d).

The metagranitoids of the Zacatepec area can be clearly linked to the Esperanza suite as discussed above. However, the correlation of the ZLGR with other lithological units of the AC is not straightforward. For instance, the ZLGR shares some similarities with the Tecomate Formation, such as the presence of marble packages or the structural position overlying the Esperanza grantoids in some sections north of the study area (Sánchez-Zavala *et al.*, 2004; Mendoza-Rosales *et al.*, 2024; Maldonado *et al.*, 2025). The general mapping of the AC also shows a belt-like continuity of the Tecomate Formation from north to south in areas east and west of Zacatepec (Figure 1). These features might suggest that the ZLGR is an extension of the Tecomate Formation, however, we argue that the rocks studied here rather belong to the pre-Pennsylvanian low-grade rocks (PPLGR) system or units, as we discuss below.

Despite the PPLGR are generally overthrusted by high-pressure rocks (c.f. Ortega-Gutiérrez et al., 2018; Figure 1), recent mapping around the Huajuapan area shows that PPLGR tend to overlie the Esperanza granitoids along undifferentiated faults or interpreted stratigraphic contacts (Mendoza-Rosales et al., 2024), a structure similar to what we describe in the Zacatepec area. The deformation styles and number of low-grade deformation events recorded in the ZLGR are also similar to these reported for other PPLGR. The pioneer work of Malone et al. (2002) described three deformation events in the Cosoltepec formation, developing fabrics analogous to what is observed in Zacatepec. Later works described similar structures in the Epazote, Las Calaveras (Hinojosa-Prieto et al., 2008), Ojo del Agua (Ramos-Arias et al., 2008), Huerta, and Salada (Morales-Gamez et al., 2009) units, and the Pitayo Lithodeme (Gonzales-Ixta, 2024); some units also show sheath folds (Ramos-Arias et al., 2008; Morales-Gamez et al., 2009). In contrast, only two deformation events have been documented for the Tecomate formation (Malone et al., 2002; Morales-Gámez et al., 2009).

Another similarity of the ZLGR and other PPLGR is the detrital zircon U-Pb age spectra, especially with the Amarillo, Zumpango units (Figure 2) and El Pitayo Lithodeme, which also present a few Mississippian-Devonian zircon grains ranging 327-385 Ma (Ortega-Obregon et al., 2009; Kirsch et al., 2014; Gonzalez-Ixta, 2024). The interpreted MDA for the Amarillo unit (339 \pm 6 Ma) even overlaps with the interpreted MDA for the ZLGR (334 ± 8.9 Ma). Contrastingly, the reported zircon U-Pb age spectra of the Tecomate Formation show a key population that is not observed in the ZLGR, or generally in the PPLGR, which is the dominant Ordovician population (Figure 2) associated with the denudation of the Esperanza granitoid (Sánchez-Zavala et al., 2004; Nance et al., 2009). It could be argued that the limited occurrence in Ordovician zircons in the ZLGR might be a consequence of the scarce availability of Ordovician zircons in the local Esperanza granitoids (Figure 10). However, the local granitoids do not seem to have contributed to the detrital populations of the ZLGR, since the ca. 1400 Ma ages observed in sample granitoid JC-2326 (Figure 10) are almost absent in metapsammite JC-2323 (Figure 2d). Thus, we contend that, with the current data, it is most likely that the ZLGR are an extension of the PPLGR outcropping in northern parts of the AC, rather than a continuation of the Tecomate Formation.

Metamorphic evolution of the low-grade rocks of the Zacatepec area

Despite the difficulty of applying phase equilibria geother-mobarometry to low-grade rocks, recent studies have been able to reproduce the observed mineral assemblages of high-variance low-grade rocks that are consistent with the geology of the area and that are validated by other geothermobarometric methods (Pò *et al.*, 2016; Franceschelli *et al.*, 2017; Balen *et al.*, 2018; Petroccia *et al.*, 2024). Such results suggest that lower-variance (more diverse mineralogy) rocks might also be ideal candidates for obtaining quantitative P-T results for low-grade complexes, assumption that we test using the rare Mnrich garnet-biotite-bearing schist of the Zacatepec area.

The first approach for phase equilibria we took considered the measured bulk rock composition of the garnet-biotite-bearing schist and it successfully reproduced the peak mineral assemblage (Figure 6b-6c) developed during D_{LG1-2} of sample JC-2310 (Figure 8a), the garnet composition of all four garnet endmembers, the TiO2 wt.% content in biotite, and the lowest SiO2 wt.% content measured in muscovite (Figure 8b). The compositional isopleths for both TiO₂ and SiO₂ in the biotite and muscovite overlap with the stability field of the interpreted peak assemblage (Figure 8b), but the intersection of the garnet isopleths falls within a mineral assemblage field where plagioclase is stable, a mineral that is not observed in the sample. This suggests that garnet growth began at 0.15-0.27 GPa and 420-450 °C, followed by an increase in pressure and temperature to 0.45 to 0.56 GPa and 470 to 510 °C (Figure 8a-8b). However, the lack of overlapping of the garnet isopleths, especially for the garnet rim composition, and the interpreted peak assemblage might also be a consequence of the change in the reactive bulk composition that evolves as garnet grows, since the elements used by garnet are no longer available for metamorphic reactions (Evans, 2004). To test this and further refine the metamorphic conditions of the sample, we extracted the composition of the garnet core, where the endmember isopleths intersect when the model predicts ca. 2.5% volume of garnet formed.

With the modified composition, the peak stability field expands to pressure values of up to 0.7 GPa (Figure 8c). The garnet composition is also well-reproduced in this model, but the intersection of the four end-members isopleths is less constrained than in the measured bulkrock composition model (Figure 8d). This intersection overlaps with the lowest portion of the peak stability field, and X_{Alm} composition falls within the peak stability field up to 0.65 GPa and 540 °C (Figure 8d). Isopleths for TiO₂ wt.% in biotite and the lowest contents of SiO₂ wt.% in muscovite also fall within the peak assemblage field (Figure 8d). The phase equilibria model with the extracted composition does not differ significantly from the original phase equilibria model, apart from the overlapping of X_{Alm} isopleths with the peak assemblage (Figure 8d) but shows that garnet growth did modify the bulk reactive composition and suggest that garnet continued growing towards the conditions of the peak assemblages, as the syn-tectonic to late syntectonic nature of the garnets show (Figure 6b). Thus, we interpret that the rock experienced an evolution from greenschist facies conditions at 0.15 to 0.27 GPa and 420 to 450 °C to upper-greenschist-lower amphibolite facies conditions at 0.45-0.65 GPa and 480 to 540 °C during D_{LG1-2} episode(s).

The interpretations of the pseudosection are validated by Ti-in-Bt thermometry that returned temperatures of 430–555 °C, which overlap with the modeled stability fields. The increase in temperature is also consistent with the garnet profiles, which show a slight increase in $X_{\rm Prp}$ and a decrease in $X_{\rm Sps}$, a typical feature of prograde garnet growth (Florence & Spear, 1991). However, the garnet-biotite thermometry returned values (391–404 °C) that do not even reach the lower temperatures obtained with the other methods. This inconsistency could be a consequence of the high spessartine contents of the garnets, that could lower temperatures (Holdaway, 2000), highlighting that this geothermometer might not be useful for low-grade Mn-rich garnets.

Our modeling of the garnet-biotite-bearing schist successfully reproduced the mineral assemblages and the composition of garnet and TiO₂ wt% content in biotite using typical phase equilibria models, demonstrating that lithologies with a low-variance mineralogy could provide geothermobarometric constraints in low-grade terranes. However, garnet-bearing rocks are rare in the PPLGR of the AC and in most low-grade metamorphic complexes. The stabilization of garnet at such low temperatures most likely occurred due to the high content of MnO (ca. 1 wt.%), which is an order of magnitude

higher (Figure 11a) than the MnO content reported for the PPLGR of the AC and the median world metapelite composition (Forshaw & Pattison, 2023). The composition of the rock could also explain the stabilization of biotite at low temperatures, since it might have been facilitated by the relatively high, K₂O, MgO, and FeO contents in JC-2310 compared to the rest of the metasedimentary rocks of the complex (Figure 11b–11d). Such anomalous composition explains why metapelitic garnets have only been reported in the Amarillo unit where amphibolite facies conditions have been inferred (Kirsch *et al.*, 2014), but not in the rest of the PPLGR that underwent greenschist facies metamorphism, and why it seems to be restricted to a small layer in the Zacatepec area (Figure 4c). However, we suggest that Mnrich garnet-bearing metapelitic layers might be common throughout the PPLGR, since sparse Mn-rich accumulations have been reported before (Ortega-Gutiérrez *et al.*, 2018).

Our P-T data could also be used as a proxy for the tectonic evolution of the PPLGR. Deformation of all the PPLGR was most likely contemporaneous, since Ar-Ar dating of separate micas from low-grade rocks in different units have returned ca. 328–346 Ma ages (Hinojosa-Prieto $et\ al.$ 2008; Ramos-Arias $et\ al.$, 2008; Ortega-Obregón $et\ al.$, 2009; Kirsch $et\ al.$, 2014; González-Ixta, 2024), which was recently confirmed to be associated to D_{LG1-2} by in-situ dating of microstructurally constraint micas (González-Ixta, 2024). The timing of the D_{LG1-2} metamorphism of the PPLGR is similar to that of

Mississippian cooling of the high-pressure rocks inferred from Ar-Ar phengite and glaucophane ages (Elías-Herrera et al., 2007), consistent with the tectonic models that suggest that the deformation and metamorphism of the PPLGR is associated to the extrusion of highpressure rocks (Hinojosa-Prieto et al. 2008; Ramos-Arias et al., 2008; Ortega-Obregón et al., 2009; Kirsch et al., 2014; González-Ixta, 2024). In this tectonic scenario, the PPLGR were accreted to the northwestern margin of Pangea. Subduction of the high-pressure suites of the AC was followed by their extrusion and exhumation, overthrusting them onto the PPLGR and causing a prograde P-T increase during D_{LG1-2} across the PPLGR. Although the metamorphic grade might have varied as suggested by the lower P-T values reported for El Pitayo Lithodeme (0.2-0.4 GPa and 260-360 °C; González-Ixta, 2024) and the inferred amphibolite conditions in the Amarillo unit (Krisch et al., 2014), our data indicates that they all might have experienced prograde history with increasing P-T conditions.

In the Zacatepec area, however, the metagranitoids are not thrusted over the low-grade rocks (Figure 3a). This structural arrangement might be a consequence of the change in the geometry of the general structure of the southern AC (Figure 1) that might have been modified by post-Mississipian tectonics, a process that has been observed in different areas of the AC (e.g., Malone et al., 2002; Morales-Gámez et al., 2009; Kirsch et al., 2014, Jaramillo-Méndez, 2015; Elías-Herrera et al., 2023).

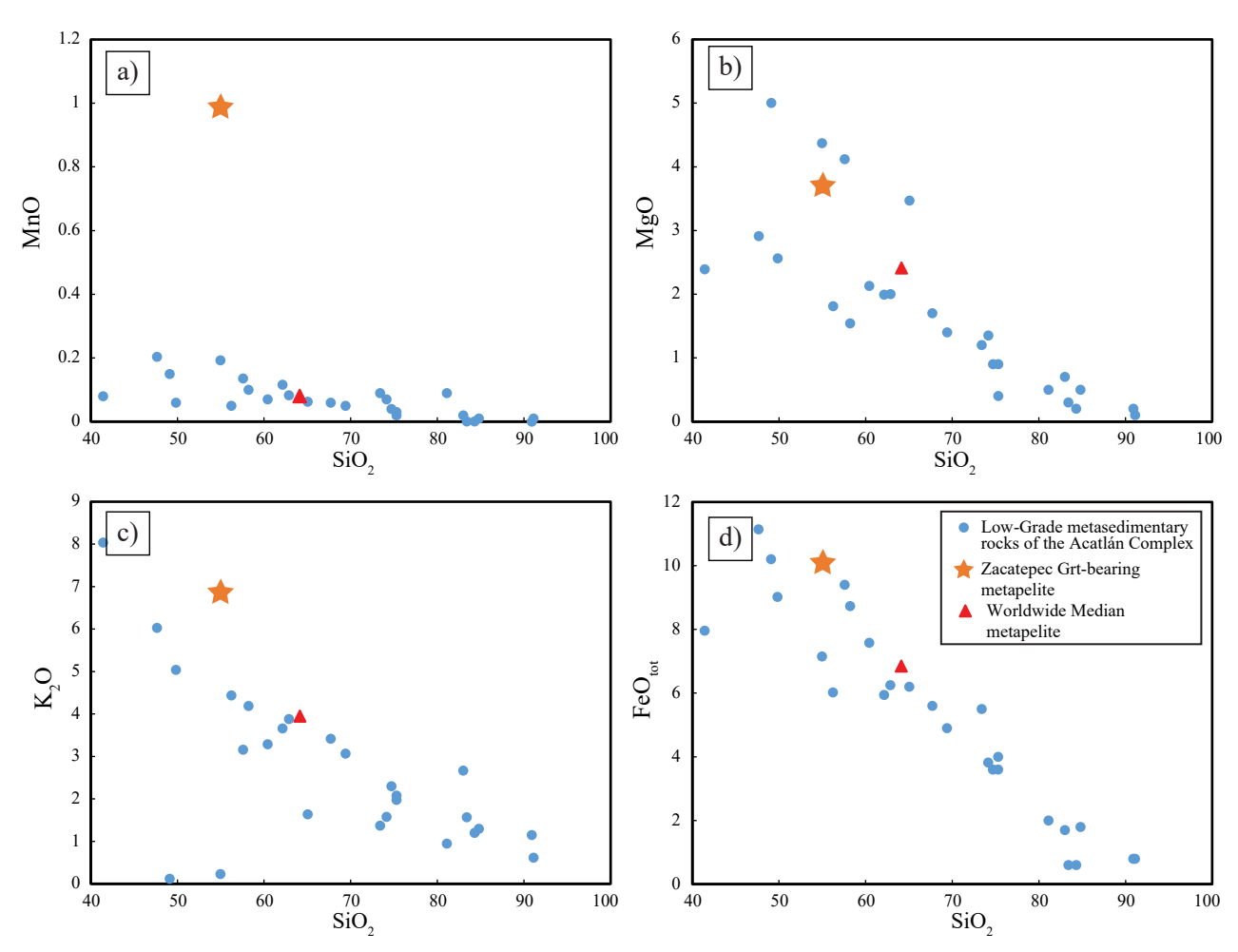


Figure 11. SiO_2 vs (a) MnO, (b) MgO, (c) K_2O and (d) FeO_{tot} diagrams showing the composition of the reported metasedimentary rocks from the pre-Pennsylvanian low-grade rocks (PPLGR) (Grodzicki *et al.*, 2008; Dostal & Keppie, 2009; Ortega-Obregón *et al.*, 2010; Kirsch *et al.*, 2014), the Zacatepec metapelite (this work) and the worldwide median metapelite composition (Forshaw and Pattison, 2023).

New constraints on the Grenvillian sources of the PPLGR and the Esperanza metagranitoids

There is a consensus that the AC evolved at the fringes of northwestern Gondwana, where the Mesoproterozoic microcontinent Oaxaquia was also located (Ortega-Gutiérrez et al., 1995; Keppie & Ortega-Gutiérrez, 2010). This paleogeography is supported by the presence of Cambrian to Neoproterozoic, as well as Proterozoic, detrital zircon ages that suggest Amazonia, the Brasiliano orogen, and the Maya block were relatively close sources (e.g., Keppie et al., 2006; Morales-Gámez et al., 2008; Nance et al., 2009). The contributions of Oaxaquia are inferred to come mainly from the Oaxacan Complex based on 1000-1200 Ma zircons (e.g., Keppie et al., 2006; Nance et al., 2009) and the proximity of the Acatlán and Oaxacan Complex. Zircons of ca. 1000-1200 Ma are abundant in the Oaxacan Complex, and the 1100-1200 Ma populations are well represented in the Zacatepec metapsammite, other low-grade metasedimentary samples across the AC (Figure 2), and the inherited zircons in the Esperanza granitoids (Figure 10) but 1000 Ma populations are generally minor or absent (Figure 2,10). Such characteristic appears to be at odds with the Oaxacan Complex as a primary source, as other non-metamorphosed sedimentary formations with clear Oaxacan provenance (e.g., the Tiñú Formation) exhibit dominant ca. 1000 ages in the detrital signal (Guerrero-Moreno et al., 2024). Moreover, flat REE zircon patterns are common in the ca. 1000 Ma Oaxacan Complex zircons, as in a large proportion of its rocks zircon crystallized contemporaneously with garnet (Solari et al., 2014, 2020), but the few grains with flat REE patterns in our samples range in ages from ca. 513-575 Ma (Figure 9e).

Recent data has shown that other Grenvillian rocks outcrop in southern Mexico, providing new alternatives to the provenance of early Neoproterozoic-Mesoproterozoic zircons described in the PPLGR and the Esperanza granitoids. Zircons recovered from rocks of El Triunfo Complex (Weber et al., 2018; Valencia-Morales et al., 2022), Sierra de Juárez Complex (Espejo-Bautista et al., 2022, 2023) and the Río Hondo Gneiss (Solari et al., 2024) have returned ages around ca. 900 Ma, 1020-1100 Ma, >1400 Ma, and more importantly a relevant occurrence of ca. 1200 Ma ages in their rocks, whereas ca. 1000 Ma zircons are not dominant (Weber et al., 2018; Espejo-Bautista et al., 2022, 2023; Valencia-Morales et al., 2022) or are even absent (Solari et al., 2024). Such <990 Ma and >1020 Ma zircon ages are found in the Zacatepec area and the larger PPLGR and Esperanza granitoids, suggesting the old continental crust involved in the formation of the Acatlán protoliths might be these recently discovered Oaxaquianrelated terranes, rather than the classic Oaxaquia basement, as it has already been suggested for the source of the Esperanza granitoids (Solari et al., 2024). Consequently, this novel interpretation of the Grenvillian-related sources of the AC rocks underscores the importance of understanding the exposure and location of classic Oaxaquia and the associated terranes during the Paleozoic.

CONCLUSIONS

Our work provides new data of a poorly explored area in the southern Acatlán Complex. We found that the Zacatepec low-grade rocks (ZLGR) were deposited in a submarine environment, with a Mississippian (334 \pm 8.9 Ma) maximum deposition age, and were later affected by three deformational events $D_{\rm LG1-3}$. These characteristics coincide with the descriptions of other pre-Pennsylvanian low-grade rocks (PPLGR), showing the ZLGR are their continuation in the southern portions of the complex. Moreover, we obtained quantitative geothermobarometric data that show that the ZLGR evolved from 0.15 to 0.27 GPa and 420 to 450 °C to 0.45–0.65 GPa and 480 to 540 °C

during the development of $D_{\rm LG1-2}$, which we propose as a proxy to the prograde evolution of the PPLGR. This metamorphic evolution is consistent with the previously proposed scenario where the low-grade metamorphism of the Acatlán Complex is associated to the overthursting of the exhumed high-pressure rocks. Furthermore, we suggest that the detrital and inherited zircon U-Pb age spectra of the low-grade rocks and Esperanza metagranitoids at Zacatepec and the rest of the Acatlán Complex indicate that non-Zapotecan Oaxaquian metamorphic terranes might have been the sources of the rocks rather than the Oaxacan Complex as commonlly interpreted. Our work shows that integral studies of low-grade rocks can provide valuable information for tectonic and paleogeographic models.

Acknowledgements. We want to thank María Consuelo Macías Romo for her help in the zircon separation and cathodoluminescence imaging, Adela Margarita Reyes Salas for her assistance with the Scanning Electronic Microscope, Carlos Ortega-Obregón for the acquisition of the U-Pb zircon data, Carlos Linares López for the microprobe data acquisition, Yessica González-Ixta for her help during fieldwork and sharing the data compilation for the low-grade rocks and Deni María San Pedro Flores for her help with thin sections preparation for microprobe analyses. We are grateful to Fernando Ortega-Gutiérrez for discussions on the area. We also thank Fausto Salazar and Eva Salazar for hosting us in their houses during fieldwork. We would like to express our gratitude to Guillermo Espejo-Bautista, Mario Alfredo Ramos-Arias and an anonymous reviewer for their constructive feedback that improved the manuscript, to Luigi Solari for editorial handling, and and to Teresa Orozco-Esquivel for the technical editing.

Author contributions. Conceptualization: Anthony Ramírez-Salazar (ARS), Joseph U. Chaverria-Urrieta (JUCU). Methodology: ARS, JUCU. Validation: ARS, JUCU Rodrigo Gutiérrez-Navarro (RGN). Investigation: ARS, JUCU. Project administration: ARS. Supervision: ARS. Visualization: ARS, JUCU, RGN. Writing - original draft: ARS, JUCU; Writing - reviewing and editing: ARS, RGN.

Data availability statement. All data supporting the findings of this contribution are available in the figures, text and supplementary material to this contribution. Supplementary Tables S1, S2, and S3 can be downloaded at the abstract's preview page of this paper

Declaration of competing interests. The authors have no conflicts of interest to declare that are relevant to the content of this article. **Funding.** This work was mainly supported by the DGAPA-UNAM PAPIIT IN105323 granted to Fernando Ortega-Gutiérrez.

SUPPLEMENTARY MATERIAL

Supplementary Tables S1 to S6 can be downloaded from the abstract's preview page of this paper at https://www.rmcg.unam.mx.

REFERENCES

Árkai, P., Faryad, S.W., Vidal, O., and Balogh, K. (2003). Very low-grade metamorphism of sedimentary rocks of the Meliata unit, Western Carpathians, Slovakia: Implications of phyllosilicate characteristics. *International Journal of Earth Sciences*, 92, 68–85. DOI: 10.1007/ s00531-002-0303-x

Balen, D., Massonne, H. J., & Lihter, I. (2018). Alpine metamorphism of low-grade schists from the Slavonian Mountains (Croatia): new P-T and geochronological constraints. *International Geology Review*, 60(3), 288–304. https://doi.org/10.1080/00206814.2017.1328710

Baltazar, O. F., & Zucchetti, M. (2007). Lithofacies associations and structural evolution of the Archean Rio das Velhas greenstone belt, Quadrilátero

- Ferrifero, Brazil: A review of the setting of gold deposits. *Ore Geology Reviews*, 32, 471–499, DOI: 10.1016/j.oregeorev.2005.03.021
- Campa, M. F., & Coney, P. J., (1983). Tectono-stratigraphic terranes and mineral resource distributions in Mexico. Canadian Journal of Earth Sciences, 20, 1040–1051.
- Cerca-Martínez, M. (2004). Deformación y magmatismo cretacico tardio terciario temprano en la zona de la plataforma Guerrero Morelos [PhD Thesis]. Universidad Nacional Autónoma de México.
- Chaverria-Urrieta J. U. (2025). Geología y petrología de la localidad de Zacatepec, Oaxaca, del Complejo Acatlán [Bachelor tesis]. Universidad Nacional Autónoma de México.
- Connolly, J. A. D. (2005). Computation of phase equilibria by linear programming: A tool for geodynamic modeling and its application to subduction zone decarbonation. *Earth and Planetary Science Letters*, 236, 524–541. DOI: 10.1016/j.epsl.2005.04.033
- Connolly, J. A. D. (2009). The geodynamic equation of state: What and how. Geochemistry, Geophysics, Geosystems, 10. DOI: 10.1029/2009GC002540
- Dostal, J., & Keppie, J. D. (2009). Geochemistry of low-grade clastic rocks in the Acatlán Complex of southern Mexico: Evidence for local provenance in felsic-intermediate igneous rocks. Sedimentary Geology, 222, 241–253. DOI: 10.1016/j.sedgeo.2009.09.011
- Elías-Herrera, M., & Ortega-Gutiérrez, F. (2002). Caltepec fault zone: An Early Permian dextral transpressional boundary between the Proterozoic Oaxacan and Paleozoic Acatlán complexes, southern Mexico, and regional tectonic implications. *Tectonics*, 21(3). DOI: 10.1029/2000tc001278
- Elías-Herrera, M., Macías-Romo, C., Sánchez-Zavala, J. L., Jaramillo-Méndez, C., Bautista-Bautista, D., Ortega-Gutiérrez, F. (2023). *Unidades metamórficas del sector oriental del Complejo Acatlán, Sur de México, en el marco de la consolidación de Pangea occidental durante el Cisuraliano-Guadalupiano*. GeoAcatlán. Complejo Acatlán 50 aniversario del inicio de las investigaciones geológicas modernas.
- Elías-Herrera, M., Macías-Romo, M. C., Ortega-Gutiérrez, F., Sánchez-Zavala, J. L., Iriondo, A., Ortega-Rivera, A. (2007). Conflicting stratigraphic and geochronologic data from the Acatlán Complex: "Ordovician" granites intrude sedimentary and metamorphic rocks of Devonian-Permian age. Eos Transactions AGU Joint Assembly Supplement, 88(23) (Abstract T41A–12).
- Elsaid, M., Aboelkhair, H., Dardier, A., Hermas, E., & Minoru, U. (2014). Processing of Multispectral ASTER Data for Mapping Alteration Minerals Zones: As an Aid for Uranium Exploration in Elmissikat-Eleridiya Granites, Central Eastern Desert, Egypt. *The Open Geology Journal*, 8(1), 69-83. https://doi.org/10.2174/1874262901408010069
- Espejo-Bautista, G., Ortega-Gutiérrez, F., Solari, L. A., Maldonado, R., & Valencia-Morales, Y. T. (2022). The Sierra de Juárez Complex: a new Gondwanan Neoproterozoic-early Palaeozoic metamorphic terrane in southern Mexico. *International Geology Review*, 64(5), 631–653. https://doi.org/10.1080/00206814.2020.1870172
- Espejo-Bautista, G., Solari, L., Maldonado, R., & Ramírez-Calderón, M. (2023). Stenian arc-magmatism and early Tonian metamorphism and anatexis along the northern border of Amazonia during the Rodinia assembly: The Pochotepec suite in southern Mexico. *Journal of South American Earth Sciences*, 124. https://doi.org/10.1016/j.jsames.2023.104248
- Estrada-Carmona, J., Weber, B., Scherer, E. E., Martens, U., & Elías-Herrera, M. (2016). Lu-Hf geochronology of Mississippian high-pressure metamorphism in the Acatlán Complex, southern México. *Gondwana Research*, 34, 174–186. DOI: 10.1016/j.gr.2015.02.016
- Evans, T. P. (2004). A method for calculating effective bulk composition modification due to crystal fractionation in garnet-bearing schist: Implications for isopleth thermobarometry. *Journal of Metamorphic Geology*, 22, 547–557. DOI: 10.1111/j.1525-1314.2004.00532.x
- Florence, F. P., & Spear, F. S. (1991). Effects of diffusional modification of garnet growth zoning on P-T path calculations. *Contributions to Mineralogy and Petrology*, 487–500.
- Forshaw, J. B., & Pattison, D. R. M. (2023). Major-element geochemistry of pelites. *Geology*, 51, 39–43, DOI: 10.1130/G50542.1
- Franceschelli, M., Battaglia, S., Cruciani, G., Pasci, S., & Puxeddu., M. (2017). Very Low-Temperature Metamorphism in Ordovician Metasedimentary

- Rocks Above and Below the Sardic Unconformity, SW Sardinia. Italy. International Journal of Earth Sciences 106, no. 2:531–548. https://doi.org/10.1007/s00531-016-1370-8
- Freeman, S.R., Inger, S., Butler, R.W.H., & Cliff, R.A., 1997, Dating deformation using Rb-Sr in white mica: Greenschist facies deformation ages from the Entrelor shear zone, Italian Alps: Tectonics, v. 16, p. 57– 76, DOI: 10.1029/96TC02477
- Galaz, E., G., Keppie, J. D., Lee, J. K. W., & Ortega-Rivera, A. (2013). A high-pressure folded klippe at Tehuitzingo on the western margin of an extrusion zone, Acatlán Complex, southern México: Gondwana Research, 23, 641–660. DOI: 10.1016/j.gr.2012.04.011
- Gómez-Tuena, A., Orozco-Esquivel, M. T., & Ferrari, L. (2007). Igneous petrogenesis of the trans-mexican volcanic belt. Special Paper of the Geological Society of America, 422, 129–181, DOI: 10.1130/2007.2422(05)
- González-Ixta, Y. (2024) Litodema El Pitayo, unidad metavolcanosedimentaria paleozoica del Complejo Acatlán, Sur de México, y su importancia en la evolución tectónica pre- y post- Pangea [Master's Thesis], Universidad Nacional Autónoma de Mëxico.
- González-Ixta, Y., & Elías-Herrera, M., (2024, April). Lithodeme El Pitayo, a Palaeozoic meta-volcanosedimentary unit of the Acatlán Complex, southern Mexico and its importance in pre-and post-Pangea tectonic evolution. EGU General Assembly Conference Abstracts (p. 368).
- Grodzicki, K. R., Nance, R. D., Keppie, J. D., Dostal, J., & Murphy, J. B. (2008). Structural, geochemical and geochronological analysis of metasedimentary and metavolcanic rocks of the Coatlaco area, Acatlán Complex, southern Mexico. *Tectonophysics*, 461, 311–323. DOI: 10.1016/j.tecto.2008.01.016
- Guerrero-Moreno, S., Solari, L. A., Maldonado, R., & Ortega-Flores, B. (2024). Detrital zircon and rutile of southern Mexico Cambrian– Ordovician sandstone: Their significance for sediment provenance and Rheic Ocean evolution. Sedimentary Geology, 469. DOI: 10.1016/j. sedgeo.2024.106665
- Gupta, R. P. (2011). Remote Sensing Geology. Berlin. Elsevier.
- Henry, D. J., Guidotti, C. V. & Thomson, J. A. (2005). The Ti-saturation surface for low-to-medium pressure metapelitic biotites: Implications for geothermometry and Ti-substitution mechanisms: *American Mineralogist*, 90, 316–328. DOI: 10.2138/am.2005.1498
- Hernández-Uribe, D. (2022) A re-evaluation of the peak P-T conditions of eclogite-facies metamorphism of the Paleozoic Acatlán Complex (Mexico) reveals deeper subduction. *Scientific Reports*, 12. DOI: 10.1038/s41598-022-25992-8
- Hernández-Uribe, D., Gutiérrez-Aguilar, F., Mattinson, C. G., Palin, R. M., & Neill, O. K. (2019). A new record of deeper and colder subduction in the Acatlán complex, Mexico: Evidence from phase equilibrium modelling and Zr-in-rutile thermometry. *Lithos*, 324–325, 551–568, DOI: 10.1016/j.lithos.2018.10.003
- Hinojosa-Prieto, H. R., Nance, R. D., Keppie, J. D., Dostal, J. V., Ortega-Rivera, A., Lee, J. K. W. (2008). Ordovician and Late Paleozoic-Early Mesozoic tectonothermal history of the La Noria area, northern Acatlán Complex, southern Mexico: Record of convergence in the Rheic and paleo-Pacific Oceans. *Tectonophysics*, 461, 324–342. DOI: 10.1016/j. tecto.2008.06.002
- Holdaway, M. J. (2000). Application of new experimental and garnet Margules data to the garnet-biotite geothermometer. *American Mineralogist*, 85, 881–892. DOI: 10.2138/am-2000-0701
- Holland, T. J. B., & Powell, R. (2011). An improved and extended internally consistent thermodynamic dataset for phases of petrological interest, involving a new equation of state for solids. *Journal of Metamorphic Geology*, 29, 333–383. DOI: 10.1111/j.1525-1314.2010.00923.x
- Holland, T. J. B., Green, E. C. R., & Powell, R. (2022). A thermodynamic model for feldspars in KAlSi3O8–NaAlSi3O8–CaAl2Si2O8 for mineral equilibrium calculations. *Journal of Metamorphic Geology*, 40, 587–600. DOI: 10.1111/jmg.12639
- Jaramillo-Méndez, C. E. (2015). Geología del Área de Caltepec-San Pedro Atzumba, Estado de Puebla [B.Sc Thesis] Instituto Politécnico Nacional.
- Keppie, J. D., & Ortega-Gutiérrez, F. (2010). 1.3-0.9 Ga Oaxaquia (Mexico): Remnant of an arc/backarc on the northern margin of Amazonia. Journal of South American Earth Sciences, 29(1), 21–27. https://doi. org/10.1016/j.jsames.2009.07.001

- Keppie, J. D., Sandberg, C. A., Miller, B. V., Sánchez-Zavala, J. L., Nance, R. D., & Poole, F. G. (2004). Implications of latest Pennsylvanian to middle permian paleontological and U-Pb SHRIMP data from the tecomate formation to re-dating tectonothermal events in the acatlán complex, Southern Mexico. *International Geology Review*, 46(8), 745–753. https://doi.org/10.2747/0020-6814.46.8.745
- Keppie, J. D., Dostal, J., Miller, B. V., Ramos-Arias, M. A., Morales-Gámez, M., Nance, R., Murphy, J. B., Ortega-Rivera, A., Lee, J. W. K., Housh, T., & Cooper, P. (2008a), Ordovician-earliest Silurian rift tholeiites in the Acatlán Complex, southern Mexico: Evidence of rifting on the southern margin of the Rheic Ocean. *Tectonophysics*, 461, 130–156. DOI: 10.1016/j.tecto.2008.01.010
- Keppie, J. D., Dostal, J., Murphy, J. B., & Nance, R. D. (2008b). Synthesis and tectonic interpretation of the westernmost Paleozoic Variscan orogen in southern Mexico: From rifted Rheic margin to active Pacific margin. *Tectonophysics*, 461, 277–290. DOI: 10.1016/j.tecto.2008.01.012
- Keppie, J. D., Nance, R. D., Fernández-Suárez, J., Storey, C. D., Jeffries, T. E., & Murphy, J. B. (2006). Detrital Zircon Data from the Eastern Mixteca Terrane, Southern Mexico: Evidence for an Ordovician—Mississippian Continental Rise and a Permo-Triassic Clastic Wedge Adjacent to Oaxaquia. *International Geology Review*, 48, 97–111. DOI: 10.2747/0020-6814.48.2.97
- Kirsch, M., Helbig, M., Duncan Keppie, J., Brendan Murphy, J., Lee, J. K. W., & Solari, L. A. (2014). A Late Triassic tectonothermal event in the eastern Acatlán Complex, southern Mexico, synchronous with a magmatic arc hiatus: The result of flat-slab subduction?. Lithosphere, 6, 63–79. DOI: 10.1130/L349.1
- Maldonado, R., Elías-Herrera, M., Espejo-Bautista, G., Ramírez-Serdán, I., Gomez-Gomez, D. E., Prado-Ordoñez, A., Macía-Romo, C. & Sánchez-Zavala, J. L. (2025). The metamorphic configuration of the Piaxtla high-pressure suite inferred from geological mapping and its metasedimentary rocks. Revista Mexicana de Ciencias Geologicas, 42(1), 17–30. doi.10.22201/igc.20072902e.2025.1.1844
- Malone, J. R., Nance, R. D., Keppie, J. D., & Dostal, J. (2002). Deformational history of part of the Acatlán Complex: Late Ordovician-Early Silurian and Early Permian orogenesis in southern Mexico: *Journal* of South American Earth Sciences, 15, 511–524. DOI: 10.1016/S0895-9811(02)00080-9
- McDonough, W. F., & Sun, S. S. (1995). The composition of the Earth. *Chemical Geology*, 120(3–4), 223–253. https://doi.org/10.1016/0009-2541(94)00140-4
- Mendoza-Rosales, C. C., Silva-Romo, G., Hernández-Marmolejo, Y. B., & Campos-Madrigal, E. (2024). Huajuapan Lithostratigraphic Map, Puebla and Oaxaca states, Mexico (E14-D14). *Journal of Maps*, 20. DOI: 10.1080/17445647.2024.2422010
- Miller, B. V., Dostal, J., Keppie, J. D., Nance, R. D., Ortega-Rivera, A., & Lee, J. K. W. (2007). Ordovician calc-alkaline granitoids in the Acatlán complex, southern México: Geochemical and geochronologic data and implications for the tectonics of the Gondwanan margin of the Rheic Ocean. Special Paper of the Geological Society of America, 423, 465–475. DOI: 10.1130/2007.2423(23)
- Morales-Gámez, M., Keppie, J. D., & Norman, M. (2008). Ordovician-Silurian rift-passive margin on the Mexican margin of the Rheic Ocean overlain by Carboniferous-Permian periarc rocks: Evidence from the eastern Acatlán Complex, southern Mexico. *Tectonophysics*, 461, 291– 310. DOI: 10.1016/j.tecto.2008.01.014
- Morales-Gámez, M., Keppie, J. D., Lee, J. K. W., & Ortega-Rivera, A. (2009). Palaeozoic structures in the Xayacatlan area, Acatlan Complex, southern Mexico: Transtensional rift- and subduction-related deformation along the margin of Oaxaquia. *International Geology Review*, 51(4), 279–303. https://doi.org/10.1080/00206810802688659
- Murphy, J. B., Keppie, J. D., Nance, R. D., Miller, B. v., Dostal, J., Middleton, M., Fernández-Suárez, J., Jeffries, T. E., & Storey, C. D. (2006). Geochemistry anbd U-Pb protolith ages of eclogitic rocks of the Asis Lithodeme, Piaxtla Suite, southern Mexico: tectonothermal activity along the southern margin of the Rheic Ocean. *Journal of the Geological Society*, 163(4), 683–695. https://doi.org/10.1144/0016-764905-108
- Nance, R. D., Miller, B. V., Keppie, J. D., Murphy, J. B., & Dostal, J. (2006).
 Acatlán Complex, southern Mexico: Record spanning the assembly and

- breakup of Pangea. Geology, 34, 857-860. DOI: 10.1130/G22642.1
- Nance, R. D., Duncan Keppie, J., Miller, B. V., Brendan Murphy, J., & Dostal, J. (2009). Palaeozoic palaeogeography of Mexico: Constraints from detrital zircon age data. *Geological Society Special Publication*, 327, 239– 269. DOI: 10.1144/SP327.12
- Napomuceno-Eslava, R. C. (2022). Análisis petrológico y microestructural el Litodema Los Lobos, facies de Esquisto Azul, Complejo Acatlán, Sur de México [Barchelor Thesis]. Instituto Politécnico Nacional.
- Olierook, H. K. H., Kirkland, C. L., Szilas, K., Hollis, J. A., Gardiner, N. J., Steenfelt, A., Jiang, Q., Yakymchuk, C., Evans, N. J., & McDonald, B. J. (2020). Differentiating between inherited and autocrystic zircon in granitoids. *Journal of Petrology*, 61(8). https://doi.org/10.1093/ petrology/egaa081
- Ortega-Gutiérrez, F. (1978). Estatigrafía del Complejo Acatlan en la Mixteca Baja, estados de Puebla y Oaxaca. *Revista Mexicana de Ciencias Geológicas*, 2, 112–131.
- Ortega-Gutiérrez, F., Ruiz, J., & Centeno-Garcia, E. (1995). Oaxaquia, a Proterozoic microcontinent accreted to North America during the late Paleozoic. *Geology*, 23, 1127–1130. DOI: 10.1130/0091-7613(1995)023<1127:OAPMAT>2.3.CO;2
- Ortega-Gutiérrez, F., Elías-Herrera, M., Reyes-Salas, M., Macías-Romo, C., & López, R. (1999). Late Ordovician-Early Silurian continental collisional orogeny in southern Mexico and its bearing on Gondwana-Laurentia connections. *Geology*, 27, 719–722. Doi:10.1130/0091-7613(1999)027<0719:LOESCC>2.3.CO;2
- Ortega-Gutiérrez, F., Elías-Herrera, M., Morán-Zenteno, D. J., Solari, L., Weber, B., & Luna-González, L. (2018). The pre-Mesozoic metamorphic basement of Mexico, 1.5 billion years of crustal evolution. *Earth-Science Reviews*, 183, 2–37. Doi:10.1016/j.earscirev.2018.03.006
- Ortega-Obregón, C., Duncan Keppie, J., Brendan Murphy, J., Lee, J. K. W., & Ortega-Rivera, A. (2009). Geology and geochronology of Paleozoic rocks in western Acatlán complex, southern Mexico: Evidence for contiguity across an extruded high-pressure belt and constraints on Paleozoic reconstructions. Bulletin of the Geological Society of America, 121, 1678–1694. DOI:10.1130/B26597.1
- Ortega-Obregon, C., Murphy, J. B., & Keppie, J. D., (2010) Geochemistry and Sm-Nd isotopic systematics of Ediacaran-Ordovician, sedimentary and bimodal igneous rocks in the western Acatlán Complex, southern Mexico: Evidence for rifting on the southern margin of the Rheic Ocean. *Lithos*, 114, 155–167. DOI:10.1016/j.lithos.2009.08.005
- Perchuk, L. L., & Lavrent'eva, I. V. (1983). Experimental investigation of exchange equilibria in the system cordierite-garnet-biotite. *Kinetics and Equilibrium in Mineral Reactions*, 199–239. DOI:10.1007/978-1-4612-5587-1_7
- Petroccia, A., Forshaw, J. B., Lanari, P., Iaccarino, S., Montomoli, C., & Carosi, R. (2024). Pressure and Temperature Estimation in Greenschist-Facies Metapelites: An Example From the Variscan Belt in Sardinia. *Journal of Metamorphic Geology*. DOI:10.1111/jmg.12799
- Pò, D. L., Braga, R., & Massonne, H. J. (2016). Petrographic, mineral and pressure-temperature constraints on phyllites from the Variscan basement at Punta Bianca, Northern Apennines, Italy. *Italian Journal of Geosciences*, 135(3), 489–502. https://doi.org/10.3301/IJG.2015.29
- Powell, W. (2003). Greenschist-facies metamorphism of the Burgess Shale and its implications for models of fossil formation and preservation. Canadian Journal of Earth Sciences, 40, 13–25. DOI:10.1139/e02-103
- Ramos-Arias, M. A., Keppie, J. D., Ortega-Rivera, A., & Lee, J. W. K., (2008). Extensional Late Paleozoic deformation on the western margin of Pangea, Patlanoaya area, Acatlán Complex, southern Mexico. *Tectonophysics*, 448, 60–76. DOI: 10.1016/j.tecto.2007.11.023
- Ramos-Arias, M. A., Keppie, J. D., Lee, J. K. W., & Ortega-Rivera, A., (2012). A Carboniferous high-pressure klippe in the western Acatlán Complex of southern México: Implications for the tectonothermal development and palaeogeography of Pangea. *International Geology Review*, 54, 779– 798. DOI: 10.1080/00206814.2011.580634
- Ruíz-Arriaga, D. (2018). Historia de la deformación de la margen oriental de la Plataforma Guerrero-Morelos [Master's Thesis]. Universidad Nacional Autonoma de Mexico.
- Sánchez-Zavala, J. L., Ortega-Gutiérrez, F., Keppie, J. D., Jenner, G. A., Belousova, E., & Maciás-Romo, C. (2004). Ordovician and

- Mesoproterozoic Zircons from the Tecomate Formation and Esperanza Granitoids, Acatlán Complex, Southern Mexico: Local Provenance in the Acatlán and Oaxacan Complexes. *International Geology Review*, 46, 1005–1021. DOI:10.2747/0020-6814.46.11.1005
- Silva-Romo, G. (2008), Guayape-Papalutla fault system: A continuous Cretaceous structure from southern Mexico to the Chortís block? Tectonic implications. *Geology*, *36*, 75–78. DOI:10.1130/G24032A.1
- Sláma, J., Košler, J., Condon, D. J., Crowley, J. L., Gerdes, A., Hanchar, J. M., Horstwood, M. S. A., Morris, G. A., Nasdala, L., Norberg, N., Schaltegger, U., Schoene, B., Tubrett, M. N., Whitehouse, M. J. (2008). Plešovice zircon A new natural reference material for U-Pb and Hf isotopic microanalysis. *Chemical Geology*, 249, 1–35. DOI: 10.1016/j. chemgeo.2007.11.005
- Solari, L. A., Gómez-Tuena, A., Bernal, J. P., Pérez-Arvizu, O., & Tanner, M. (2010). U-Pb zircon geochronology with an integrated la-icp-ms microanalytical workstation: Achievements in precision and accuracy. Geostandards and Geoanalytical Research, 34, 5–18. DOI: 10.1111/j.1751-908X.2009.00027.x
- Solari, L. A., Ortega-Gutiérrez, F., Elías-Herrera, M., Ortega-Obregón, C., Macías-Romo, C., & Reyes-Salas, M. (2014). Detrital provenance of the Grenvillian Oaxacan Complex, southern Mexico: A zircon perspective. *International Journal of Earth Sciences*, 103, 1301–1315. DOI: 10.1007/ s00531-013-0938-9
- Solari, L. A., Ortega-Obregón, C., Ortega-Gutiérrez, F., & Elías-Herrera, M. (2020). Origin and evolution of the Grenvillian Oaxacan Complex, southern Mexico: Hf isotopic and U-Pb geochronologic constraints. In U. C., Martens, R. S Molina-Garza (eds.), Southern and Central Mexico: Basement Framework, Tectonic Evolution, and Provenance of Mesozoic-Cenozoic Basins, 546. Geological Society of America. DOI: 10.1130/2020.2546(03)
- Solari, L., Elías-Herrera, M., Espejo-Bautista, G., Jaramillo-Jaramillo, M., Macías-Romero, M.C., & Ortega-Obregón, C. (2024). U-Pb geochronology and Hf isotopes of the Grenvillian Río Hondo gneisses, Puebla: Redefining the western edge of Oaxaquia. Revista Mexicana de Ciencias Geológicas, 41(1), 87–102. https://doi.org/10.22201/cgeo.20072902e.2024.1.1760
- Talavera-Mendoza, O., Ruiz, J., Gehrels, G.E., Meza-Figueroa, D.M., Vega-Granillo, R., and Campa-Uranga, M.F. (2005). U-Pb geochronology of the Acatlán Complex and implications for the Paleozoic paleogeography and tectonic evolution of southern Mexico. *Earth and Planetary Science Letters*, 235, 682–699. DOI: 10.1016/j.epsl.2005.04.013
- Thornbury, F. (1969) *Principles of Geomorphology*. 2nd ed, London: Willey Tolson, G. (2005). La falla Chacalapa en el sur de Oaxaca. *Boletín de la Sociedad Geológica Mexicana*, 111–122.
- Torres Carbonell, P.J., Cao, S.J., and Dimieri, L. V. (2017). Spatial and temporal characterization of progressive deformation during orogenic growth: Example from the Fuegian Andes, southern Argentina. *Journal* of Structural Geology, 99, 1–19. DOI: 10.1016/j.jsg.2017.04.003

- Torres de León, H. R. (2005). Geología, Estructuras y tectónica en el Área de la Venta, Guerrero [Master's Thesis]. Universidad Nacional Autónoma de México.
- Valencia-Morales, Y. T., Weber, B., Tazzo-Rangel, M. D., González-Guzmán, R., Frei, D., Quintana-Delgado, J. A., & Rivera-Moreno, E. N. (2022). Early Mesoproterozoic inliers in the Chiapas Massif Complex of southern Mexico: Implications on Oaxaquia-Amazonia-Baltica configuration. *Precambrian Research*, 373. https://doi.org/10.1016/j.precamres.2022.106611
- Vega-Granillo, R., Talavera-Mendoza, O., Meza-Figueroa, D., Ruiz, J., Gehrels, G.E., López-Martínez, M., and de la Cruz-Vargas, J.C. (2007). Pressure-temperature-time evolution of Paleozoic high-pressure rocks of the Acatlán Complex (southern Mexico): Implications for the evolution of the Iapetus and Rheic Oceans. Bulletin of the Geological Society of America, 119, 1249–1264. DOI: 10.1130/B226031.1
- Vermeesch, P. (2018). IsoplotR: A free and open toolbox for geochronology. Geoscience Frontiers, 9, 1479–1493. DOI: 10.1016/j.gsf.2018.04.001
- Weber, B., González-Guzmán, R., Manjarrez-Juárez, R., Cisneros de León, A., Martens, U., Solari, L., Hecht, L., & Valencia, V. (2018). Late Mesoproterozoic to Early Paleozoic history of metamorphic basement from the southeastern Chiapas Massif Complex, Mexico, and implications for the evolution of NW Gondwana. *Lithos*, 300–301, 177–199. https://doi.org/10.1016/j.lithos.2017.12.009
- Wiedenbeck, M. A. P. C., Alle, P., Corfu, F. Y., Griffin, W. L., Meier, M., Oberli, F. V., et al. (1995). Three natural zircon standards for U-Th-Pb, Lu-Hf, trace element and REE analyses. *Geostandards Newsletter*, 19(1), 1–23. https://doi.org/10.1111/j.1751-908X.1995.tb00147.x
- White, R. W., Powell, R., Holland, T. J. B., Johnson, T. E., & Green, E. C. R. (2014), New mineral activity-composition relations for thermodynamic calculations in metapelitic systems. *Journal of Metamorphic Geology*, 32, 261–286. DOI: 10.1111/jmg.12071
- Whitney, D. L., & Evans, B. W. (2010). Abbreviations for names of rock-forming minerals. American Mineralogist, 95(1), 185–187. https://doi.org/10.2138/am.2010.3371
- Yañez, P., Ruiz, J., Patchett, P. J., Ortega-Gutiérrez, F., & Gehrels, G. E. (1991). Isotopic studies of the Acatlan Complex, southern Mexico: implications for Paleozoic North American tectonics. *Geological Society of America Bulletin*, 103, 817–828. DOI: 10.1130/0016-7606(1991)103<0817:ISOT AC>2.3.CO;2
- Zheng, Y. F., Zhou, J. B., Wu, Y. B., & Xie, Z. (2005). Low-grade metamorphic rocks in the dabie-sulu orogenic belt: A passive-margin accretionary wedge deformed during continent subduction. *International Geology Review*, 47, 851–871. DOI: 10.2747/0020-6814.47.8.851